J. Smidt, and A. Mehlkopf, private communication.
E. Van der Drift, A. F. Mehlkopf, and J. Smidt, *Chem. Phys. Lett.* **36**, 385 (1975).
M. M. Dorio and J. C. W. Chien, *Macromolecules* **8**, 734 (1975); M. M. Dorio, and J. C. W. Chien, *J. Chem. Phys.* **62**, 3963 (1975); M. M. Dorio, Ph.D. thesis, University of Massachusetts, Amherst (1975).
M. Smigel, L. Dalton, J. Hyde, and L. Dalton, *Proc. Natl. Acad. Sci.* **71**, 1925 (1974).
J. S. Hyde, M. Smigel, L. Dalton, and L. Dalton, *J. Chem. Phys.* **62**, 1655 (1975).

3

Theory of Multiple Resonance and ESR Saturation in Liquids and Related Media

Jack H. Freed

1. *Introduction to Saturation*

1.1. *General Considerations*

The well-known result from the steady-state solution of the Bloch equations is that the absorption is given by the y component of magnetization $\tilde{M}_y$ in the rotating frame[1]:

$$\tilde{M}_y = \frac{\gamma H_1 T_2}{1 + (T_2\,\Delta\omega)^2 + \gamma_e^2 \beta_1^2 T_1 T_2} M_0 \tag{1}$$

with M_0 the equilibrium magnetization, β_1 the strength of the rf magnetic field, and γ_e the electron-spin gyromagnetic ratio. When we switch to a quantum mechanical description, we can calculate

$$M_\pm = M_x \pm iM_y = (\tilde{M}_x \pm i\tilde{M}_y)e^{\pm i\omega t} \tag{2}$$

statistically from its associated quantum mechanical operator

$$\mathcal{M}_\pm = \mathcal{N} h\gamma_e S_\pm \tag{3}$$

where $\mathcal{N}$ is the concentration of electron spins, by taking a trace of the spin density matrix $\sigma(t)$ with the spin operator $S_\pm$:

$$M_\pm(t) = \mathcal{N} h\gamma_e \operatorname{Tr} \sigma(t) S_\pm \tag{4}$$

The trace is invariant to a choice of zero-order basis states.

Jack H. Freed • Department of Chemistry, Cornell University, Ithaca, New York

The basis of our analysis here will be the equation of motion for $\sigma(t)$ appropriate in the motional narrowing region, which has been derived in several places.[1-3] That is, we write in operator form

$$\dot{\sigma} = -i[\mathscr{H}_0 + \varepsilon(t), \sigma] + R(\sigma - \sigma_{eq}) \tag{5a}$$

which may be rewritten in terms of matrix elements as

$$\dot{\sigma}_{\alpha\alpha'}(t) = -i\omega_{\alpha\alpha}\sigma_{\alpha\alpha'} - i[\varepsilon(t), \sigma]_{\alpha\alpha'} + \sum_{\beta\beta'} R_{\alpha\alpha'\beta\beta'}(\sigma_{\beta\beta'} - \sigma_{eq\beta\beta'}) \tag{5b}$$

where $\mathscr{H}_0$ is the zero-order spin Hamiltonian leading to the resonant transition frequencies $\omega_{\alpha\alpha'}$ between eigenstates α and α', $\varepsilon(t)$ includes the interaction of the spins with the various oscillating rf and microwave fields, which induce the resonances as well as any high-frequency modulation of the dc field, while R is the relaxation matrix with elements $R_{\alpha\alpha'\beta\beta'}$. The relaxation matrix yields the linewidths and the transition probabilities for relaxation from nonequilibrium population distributions. It is clear, from the form of equations (5) that in order to get stable exponential relaxation, we must require that the real part of $R_{\alpha\alpha'\beta\beta'}$ be negative (i.e., Re $R < 0$). We will give simple examples of the use of the relaxation matrix below. The inclusion of the equilibrium density matrix σ_{eq} in equations (5) is part of a high-temperature approximation for which we write

$$\sigma_{eq} = \frac{\exp(-\hbar\mathscr{H}_0/kT)}{\mathrm{Tr}[\exp(-\hbar\mathscr{H}_0/kT)]} \approx \frac{1}{A}\left(1 - \frac{\hbar\mathscr{H}_0}{kT}\right) \tag{6}$$

where A is the total number of spin eigenstates and k is Boltzmann's constant.

1.2. *A Simple Line: Two-Level System*

We have from equation (5b) that when $E(t) = 0$ and $R = 0$, then

$$\sigma_{\alpha\alpha'}(t) = \exp(-i\omega_{\alpha\alpha'}t)\sigma_{\alpha\alpha'}(0) \tag{7}$$

Thus, if $\sigma_{\alpha\alpha'}(0) \neq 0$, then $\sigma_{\alpha\alpha'}(t)$ will be oscillatory. Now suppose we have only a simple line with $\omega_0 = \omega_{ab}$, where a and b are the $M_s = \frac{1}{2}$ and $-\frac{1}{2}$ levels, and there are no other spin levels. Then

$$\langle b|S_-|a\rangle = \langle a|S_+|b\rangle = 1 \tag{8}$$

and

$$\mathrm{Tr}[\sigma(t)S_+] = \sigma(t)_{ba}S_{+ab} = \sigma(t)_{ba} \tag{9}$$

with

$$\sigma_{ba}(t) = \exp[(-i\omega_{ba} + R_{ba,\,ba})t]\sigma_{ba}(0) \tag{10}$$

We have in equation (10) included only the "diagonal" element of this four-indexed variable. In this form, we see that $-R_{ba,\,ba} = T_2^{-1}$ for this simple line whose relaxation is uncoupled to any other lines. Since Re R is negative, $\sigma_{ba} \to 0$ for $t \gg |\mathrm{Re}\,R|^{-1}$. Thus, there will be no steady-state absorption unless we include effects of the rf field. So we add to the Hamiltonian

$$\hbar\varepsilon(t) = \tfrac{1}{2}\hbar\gamma_e B_1[S_+ e^{-i\omega t} + S_- e^{+i\omega t}] \tag{11}$$

which is the interaction of the spin with a rotating field $\mathbf{B}_1 = B_1(\cos\omega t\mathbf{i} + \sin\omega t\mathbf{j})$. Then for our simple line the $\langle b| - |a\rangle$ matrix element of equation (5a) is

$$\dot{\sigma}_{ba} = (i\omega_0 + R_{ba,\,ba})\sigma_{ba} - id(\sigma_{bb} - \sigma_{aa})e^{i\omega t} \tag{12}$$

where

$$d = \tfrac{1}{2}\gamma_e B_1\langle b|S_-|a\rangle = \tfrac{1}{2}\gamma_e B_1 \tag{13}$$

Now the power absorbed from the rotating field is just[1]:

$$P = \omega B_1 \tilde{M}_y = \frac{-\omega B_1 i}{2}(M_+ e^{-i\omega t} - M_- e^{i\omega t}) \tag{14}$$

where from equation (4) $M_\pm \propto \mathrm{Tr}_\sigma[\sigma(t)S_\pm]$ and S_{+ab} requires $\sigma(t)_{ba}$ in the trace. Thus, only the component of $\sigma(t)_{ba}$ oscillating as $e^{i\omega t}$ will give a net time-averaged power absorption. So, let

$$\sigma_{ba} = Ze^{i\omega t} \tag{15}$$

and assume Z is time independent to achieve the steady-state solution. [More rigorously, the steady state σ_{ba} may be expanded in Fourier components $n\omega$, where $n = 0, 1, 2, \ldots$, but only the component oscillating at frequency ω need be considered (see Freed *et al.*[5]).] Thus we have

$$(\Delta\omega + iR_{ba,\,ba})Z = d(\sigma_{bb} - \sigma_{aa}) \tag{16}$$

where $(\sigma_{bb} - \sigma_{aa})$ is the population difference in the two states. Now note that σ is Hermitian, so $\sigma_{ab} = \sigma_{ba}^*$ and

$$\sigma_{ab}^* = Z^* e^{-i\omega t} \tag{17}$$

Thus,

$$P \propto \mathrm{Im}\,Z \equiv Z'' \tag{18}$$

We may begin to suspect that Z plays the role of $\tilde{M}_+$ (while Z^* is $\tilde{M}_-$). Also, we have already noted that

$$R_{ba,\,ba} = -(1/T_2)_{ba} = -(1/T_2)_{ab}$$

We now need the diagonal spin-density matrix elements σ_{bb} and σ_{aa}, which in steady state are not oscillating in time. We get from equation (5b),

$$R_{aa,\,aa}\sigma_{aa} + R_{aa,\,bb}\sigma_{bb} = di(Z - Z^*) = -2d\,\mathrm{Im}\,Z \tag{19a}$$

$$R_{bb,\,aa}\sigma_{aa} + R_{bb,\,bb}\sigma_{bb} = 2d\,\mathrm{Im}\,Z \tag{19b}$$

Here we see that $R_{aa,\,bb}$ and $R_{bb,\,aa}$ play the role of transition probabilities. Thus, we may write

$$R_{aa,\,bb} = R_{bb,\,aa} = W_{ab} = W_{ba} \tag{20a}$$

while

$$R_{aa,\,aa} = -\sum_{\gamma \neq a} W_{a\gamma} \tag{20b}$$

where W_{ab} is the transition probability from state b to state a, which leads to spin relaxation. Note that in the high-temperature approximation, $W_{ab} = W_{ba}$; i.e., the matrix formed from the transition probabilities is symmetric.

For simplicity, let $\gamma = b$ only (i.e., our simple line). Then we have

$$W_{ab}(\chi_a - \chi_b) = 2dZ'' \tag{21}$$

where

$$\chi_a \equiv \sigma_{aa} - \sigma_{eqaa} \tag{22a}$$

$$\chi_b \equiv \sigma_{bb} - \sigma_{eqbb} \tag{22b}$$

so that the effect of the W_{ab} etc., is to lead to thermal equilibrium [cf. equation (6)] in the absence of $\varepsilon(t)$. Now equation (16) is rewritten as

$$(\Delta\omega - iT_2^{-1})Z + d(\chi_a - \chi_b) = q\omega_0 d \tag{23}$$

where the high-temperature approximation [cf. equation (6)]

$$\sigma_{eqaa} - \sigma_{eqbb} \cong \frac{\exp(-E_a/kT) - \exp(-E_b/kT)}{\sum_\alpha \exp(-E_\alpha/kT)} \cong \frac{-\hbar\omega_{ab}}{kTA} \equiv -q\omega_0 \tag{24}$$

has been used. Here, A, the number of spin states, is 2 in our example. We now need to solve the coupled equation

$$\begin{pmatrix} \Delta\omega & T_2^{-1} & d \\ -T_2^{-1} & \Delta\omega & 0 \\ 0 & -2d & W_{ab} \end{pmatrix} \begin{pmatrix} Z' \\ Z'' \\ \chi_a - \chi_b \end{pmatrix} = \begin{pmatrix} q\omega_0 d \\ 0 \\ 0 \end{pmatrix} \tag{25}$$

This gives:

$$Z' = \Delta\omega\, T_2 Z'' \tag{26a}$$

$$Z'' = \frac{qd\omega_0 T_2}{1 + \Delta\omega^2\, T_2^2 + 4d^2 T_2 T_1} \tag{26b}$$

where $T_1 \equiv (2W_e)^{-1}$ and

$$(\chi_a - \chi_b) = q\omega_0 4d^2 \frac{T_2 T_1}{1 + \Delta\omega^2 T_2^2 + 4d^2 T_2 T_1} \tag{26c}$$

These results are very similar to steady-state solutions of the Bloch equations, and we can get correspondence if

$$2M_0 = q\omega_0 = \frac{\hbar\omega_0}{AkT} = \sigma_{eqaa} - \sigma_{eqbb} \tag{27a}$$

$$T_2 = (T_2)_{ab}, \qquad T_1 = (T_1)_{ab} \tag{27b}$$

$$\gamma\mathbf{B} = -\omega_0\mathbf{k} + 2|d|(\mathbf{i}\cos\omega t + \mathbf{j}\sin\omega t) \tag{27c}$$

$$Z' = \tilde{M}_x, \qquad Z'' = \tilde{M}_y, \qquad Z = \tilde{M}_+ \tag{27d}$$

$$\chi_a - \chi_b = 2(M_0 - M_z) \tag{27e}$$

The above treatment is based on the high-field approximation $\omega_0/\gamma_e \equiv |B_0| \gg |B_1|$, as well as the fast motional condition $|\mathscr{H}_1|\tau_c \ll 1$, where $\mathscr{H}_1(t)$ is the random perturbation leading to the relaxation matrix $R_{\alpha\alpha'\beta\beta'} \sim \tau_c$ is the relaxation time for the random process modulating $\mathscr{H}_1(t)$, and this second inequality is the basis of the motional narrowing expression equation (5) for σ.[1-5] It also requires that $|\gamma B_1|\tau_c \ll 1$ in order that the **R** not be significantly affected by the presence of the rf field.[1,5]

1.3. *A Simple Line: Multilevel System*

The next most complicated case is a simple line coupled by relaxation to other spin eigenstates (see Figure 1). We now have

$$\sum_{\alpha \neq a} W_{a\alpha}(\chi_a - \chi_\alpha) = 2d\,\mathrm{Im}\,Z \tag{28a}$$

$$\sum_{\alpha \neq b} W_{b\alpha}(\chi_b - \chi_\alpha) = -2d\,\mathrm{Im}\,Z \tag{28b}$$

And, for $\alpha \neq a, b$, we get $A - 2$ equations

$$\sum_{\alpha}{}' W_{\alpha\beta}(\chi_\alpha - \chi_\beta) = 0, \qquad \beta \neq \alpha \tag{28c}$$

In equation (28c), we have assumed all transitions other than $a \to b$ are too far off resonance to have any appreciable off-diagonal density matrix elements; i.e., they are not excited by the rf field. Note that we can rewrite equation (23) as

$$Z = \frac{d[\omega_0 q - (\chi_a - \chi_b)]}{\Delta\omega - iT_2^{-1}} \tag{23'}$$

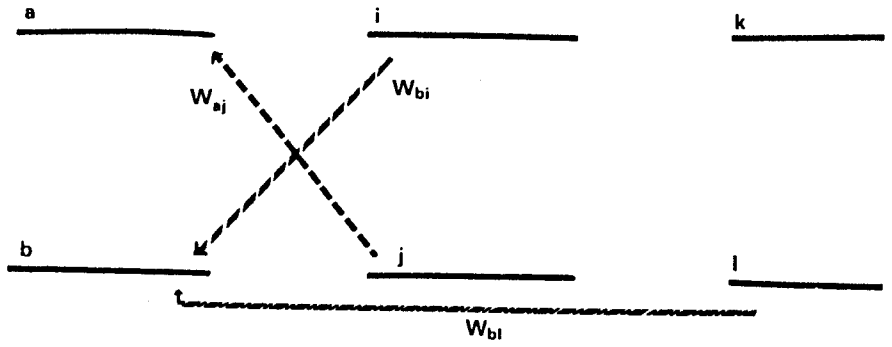

Figure 1. The pair of states corresponding to a simple line that are coupled by relaxation to other spin eigenstates.

When $\Delta\omega$ is very large, then $Z \to 0$ as $(d/\Delta\omega) \to 0$. In discussing this limit, we shall often use the convenient artifact of letting $d \to 0$ for that transition instead of more rigorously letting $(1/\Delta\omega) \to 0$.

The conservation of probability is

$$\mathrm{Tr}\,\sigma = \mathrm{Tr}\,\sigma_{eq} = 1 \qquad \text{or} \qquad \mathrm{Tr}\,\chi = 0 \tag{29}$$

This is needed, because the above set of A equations are not all linearly independent. We can write these A equations in matrix notation as[6]:

$$\mathbf{W}\chi = \mathbf{U} \tag{30}$$

with $U_a = -U_b = 2d\ \mathrm{Im}\ Z$. When the rank of $\mathbf{W}$ is $A - 1$, then replacement of any one equation by equation (29) yields the matrix $\mathbf{W}^l$, which is now nonsingular, and we have

$$\chi = (\mathbf{W}^l)^{-1}\mathbf{U}^l \tag{30'}$$

Proper solutions of this $\mathbf{W}$ inversion are crucial in all saturation and double resonance analyses. It is possible to obtain general solutions by taking advantage of the general properties of $\mathbf{W}$ as developed in the Appendix.[6,7]

$$(\chi_a - \chi_b) = \Omega_{ba,\,ba} V_{ba}[q\omega_0 - (\chi_a - \chi_b)] \tag{31}$$

where from equations (16) and (22)

$$dZ'' = V_{ba}[q\omega_0 - (\chi_a - \chi_b)] \tag{32}$$

with

$$V_{ba} \equiv 2d^2 T_2/(1 + T_2^2\,\Delta\omega^2) \tag{33}$$

and

$$\Omega_{ba,\,ba} \equiv 2C_{ba,\,ba}/C \tag{34}$$

where C is any cofactor of $\mathbf{W}$ (they are all equal, as may be shown from the properties of $\mathbf{W}^l$), and $C_{ba,\,ba}$ is the double cofactor of $\mathbf{W}$ obtained as the (signed) determinant resulting when the ath and bth rows and columns are deleted from $\mathbf{W}$ (see the Appendix).[6] More generally, we write

$$\Omega_{ij,\,kl} \equiv 2C_{ij,\,kl}/C \tag{35a}$$

where $C_{ij,\,kl}$ is the double cofactor of $\mathbf{W}$ obtained by deleting the ith and jth rows and the kth and lth columns of $\mathbf{W}$ and giving it the correct sign (cf. the Appendix).

The proof of equation (31) from equation (30') is as follows. First we note that equation (30') may be rewritten as

$$\chi_i = \sum_k (C^l_{ki}/|\mathbf{W}^l|)U^l_k \tag{36}$$

where C^l_{ki} is the kith cofactor of $\mathbf{W}^l$. Now

$$|\mathbf{W}^l| = \sum_k C_{lk} = AC \tag{37}$$

where the second equality follows from identity (1) in the Appendix [equation (A.22)]. Now, for this case of a single transition, we have

$$\begin{aligned}(\chi_a - \chi_b) &= \frac{1}{AC}\sum_k (C^l_{ka} - C^l_{kb})U^l_k \\ &= \frac{1}{C}\sum_k C_{kl,\,ab}U^l_k = \sum_k \Omega_{kl,\,ab}U^l_k/2\end{aligned} \tag{38}$$

where identity (3) of the Appendix has been used. We now recognize that only $U_a = -U_b$ are nonzero, and since l is arbitrary, we let $l = b$ to yield equation (31).

The net result is to obtain our earlier results of equation (26), but now,

$$T_1 \to \tfrac{1}{4}\Omega_{ba,\,ba} \equiv \tfrac{1}{4}\Omega_{ba} \tag{39}$$

where Ω_{ba} is the saturation parameter for the $b \leftrightarrow a$ transition. It is not a simple T_1 nor decay time. In fact, there are as many as $(A - 1)$ different nonzero decay constants in the transient solution (which come from diagonalizing the $\mathbf{W}$ matrix). This Ω_{ba} may be regarded as a steady-state self-impedance representing the response of the $b \leftrightarrow a$ transition to the application of an rf field. That is, we rewrite equations (31) and (32) as

$$(\chi_a - \chi_b) = \Omega_{ba} \cdot (dZ'') \tag{40}$$

and make the electrical circuit analogy by letting $(\chi_a - \chi_b) = E$, $\Omega_{ba} = R$, and $dZ'' = I$. Thus, we see that inducing a resonant transition is formally equivalent to inducing a current flow, which causes a voltage drop $(\chi_a - \chi_b)$ proportional to the resistance Ω_{ba}.

2. ELDOR

Now we introduce a second ESR microwave field. Assume there are only two transitions of interest (see Figure 2). Now we have

$$\varepsilon(t) = \tfrac{1}{2}\gamma_e B_o[S_+ \exp(-i\omega_o t) + S_- \exp(+i\omega_o t)] + \tfrac{1}{2}\gamma_e B_p[S_+ \exp(-i\omega_p t) + S_- \exp(+i\omega_p t)] \tag{41}$$

where o and p refer to observing and pumping modes, respectively. We are looking to the applied fields to generate steady-state off-diagonal density matrix elements as a result of the resonance phenomena. We assume

$$|\gamma_e B_o|,\ |\gamma_e B_p|,\ |R| \ll |\omega_{aa'} - \omega_{bb'}| \sim |a| \tag{42}$$

so the hyperfine lines always remain well separated. Then we may have $\omega_{aa'} - \omega_o = -\Delta\omega_o \sim 0$, while $|\omega_{aa'} - \omega_p| \sim |a|$ and $\omega_{bb'} - \omega_p = -\Delta\omega_p \sim 0$, while $|\omega_{bb'} - \omega_o| \sim |a|$. Thus, the important elements are:

$$\sigma_{a'a} = \chi_{a'a} = Z_{a'a}\exp(i\omega_o t) \equiv Z_o \exp(i\omega_o t) \tag{43a}$$

$$\sigma_{b'b} = \chi_{b'b} = Z_{b'b}\exp(i\omega_p t) \equiv Z_p \exp(i\omega_p t) \tag{43b}$$

We obtain from equation (5)

$$(\Delta\omega_o - i/T_{2,o})Z_o + d_o(\chi_a - \chi_{a'}) = q\omega_{aa'}d_o \cong q\omega_e d_o \tag{44a}$$

$$(\Delta\omega_p - i/T_{2,p})Z_p + d_p(\chi_b - \chi_{b'}) = q\omega_{bb'}d_p \cong q\omega_e d_p \tag{44b}$$

Also, the analogs of equations (28) are now

$$\sum_{\alpha \neq a} W_{a\alpha}(\chi_a - \chi_\alpha) = 2d_o Z_o'' \tag{45a}$$

$$\sum_{\alpha \neq a'} W_{a'\alpha}(\chi_{a'} - \chi_\alpha) = -2d_o Z_o'' \tag{45b}$$

$$\sum_{\alpha \neq b} W_{b\alpha}(\chi_b - \chi_\alpha) = 2d_p Z_p'' \tag{45c}$$

$$\sum_{\alpha \neq b'} W_{b'\alpha}(\chi_{b'} - \chi_\alpha) = -2d_p Z_o'' \tag{45d}$$

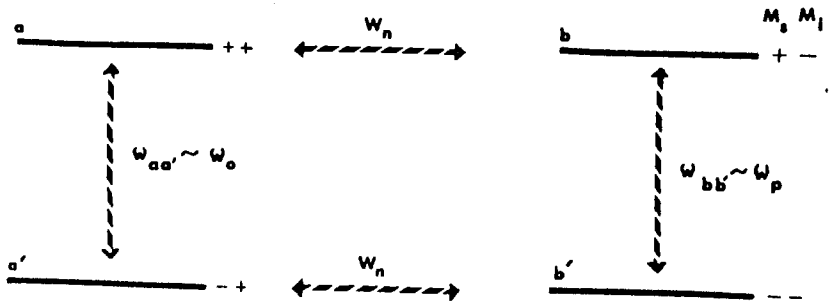

Figure 2. Example of ELDOR being performed on a simple four-level system.

These equations may be rewritten in matrix form as

$$(\mathbf{K} + i\mathbf{R})\mathbf{Z} = \mathbf{d}\chi + \mathbf{Q} \tag{46a}$$

$$(\mathbf{W}^j)(\chi) = -2\mathbf{d}^{tr\,j}\mathbf{Z}'' \tag{46b}$$

where

$$\mathbf{Q} \cong q\omega_e \begin{pmatrix} d_o \\ d_p \end{pmatrix} \tag{47a}$$

$$\mathbf{K} = \begin{pmatrix} \Delta\omega_o & 0 \\ 0 & \Delta\omega_p \end{pmatrix} \tag{47b}$$

$$-\mathbf{R} = \begin{pmatrix} T_{2,o}^{-1} & 0 \\ 0 & T_{2,p}^{-1} \end{pmatrix} \tag{47c}$$

$$-\mathbf{d} = \begin{pmatrix} d_o & -d_o & 0 & 0 \\ 0 & 0 & d_p & -d_p \end{pmatrix} \tag{47d}$$

$\mathbf{W}^j$ is a 4×4 transition probability matrix in the space of the four spin eigenstates with the jth row replaced by ones, and $\mathbf{d}^{tr\,j}$ is the transpose of $\mathbf{d}$ with the jth row replaced by zero. $\mathbf{Z}$ is a vector in the two-dimensional space of induced transitions. The formal solution is given by

$$\mathbf{Z}'' = \mathbf{M}^{-1}(-\mathbf{R}^{-1})\mathbf{Q} \tag{48a}$$

$$\mathbf{Z}' = (-\mathbf{R}^{-1})\mathbf{K}\mathbf{Z}'' \tag{48b}$$

$$\mathbf{d}\chi = -\mathbf{S}\mathbf{Z}'' \tag{48c}$$

where

$$\mathbf{M} = \mathbf{1} + (\mathbf{R}^{-1}\mathbf{K})^2 + (-\mathbf{R}^{-1})\mathbf{S} \tag{49a}$$

and

$$\mathbf{S} = 2[\mathbf{D}(\mathbf{W}^j)^{-1}\mathbf{D}^{tr\,j}] \tag{49b}$$

Suppose $d_p = 0$. One recovers the single-line, simple saturation result, and by comparison, we find

$$S_{o,o} = d_o^2\Omega_{aa',aa'} \equiv d_o^2\Omega_{o,o} \tag{50}$$

One finds more generally (cf. Section 6.2.2 and the Appendix),

$$S_{\lambda,\eta} = d_\lambda d_\eta \Omega_{\lambda,\eta} \tag{51}$$

where $\Omega_{\lambda,\eta}$ is a cross-impedance (cross-saturation parameter), which is determined solely by the spin relaxation processes and represents the impedance at transition i from an external disturbance (e.g., a resonant rf field) on the transition j. [It is obtained by equation (35a) with $i \to j$ being the λth transition and $k \to l$ the ηth transition.]

Thus, equation (48c) is a generalization of equation (40) for the single resonance case. In fact, it gives

$$(\chi_a - \chi_{a'}) = d_o\Omega_{o,o}Z_o'' + d_p\Omega_{o,p}Z_p'' \tag{52a}$$

$$(\chi_b - \chi_{b'}) = d_p\Omega_{p,p}Z_p'' + d_o\Omega_{p,o}Z_o''. \tag{52b}$$

with an electrical circuit analogy similar to that of equation (40). It follows from equations (47)–(51) that

$$\mathbf{M} = \begin{pmatrix} 1 + \Delta\omega_o^2 T_{2,o}^2 + d_o^2 T_o \Omega_o & d_o d_p \Omega_{o,p} T_{2,o} \\ d_p d_o \Omega_{p,o} T_{2,p} & 1 + \Delta\omega_p^2 T_{2,p}^2 + d_p^2 T_{2,p}\Omega_p \end{pmatrix} \tag{53}$$

where we have let $\Omega_{o,o} = \Omega_o$ and $\Omega_{p,p} = \Omega_p$. Then, from equation (48a),

$$Z_o'' = q\omega_e T_{2,o} d_o \frac{1 - \xi_o/\Omega_{p,o}}{1 + \Delta\omega_o^2 T_{2,o}^2 + d_o^2 T_{2,o}(\Omega_o - \xi_o)} \tag{54}$$

with

$$\xi_o = d_p^2 T_{2,p}\Omega_{o,p}\Omega_{p,o}/(1 + \Delta\omega_p^2 T_{2,p}^2 + d_p^2 T_{2,p}\Omega_p) \tag{54'}$$

Now consider some special cases. Let us have $\Delta\omega_p = 0$ (represented by a superscript r) and very strong saturation of the pump mode:

$$d_p^2 T_p \Omega_p \gg 1 \tag{55}$$

(where we are now dropping the subscript 2 on the various T_2). Then

$$\xi_o^r(d_p^2 \to \infty) = \Omega_{o,p}\Omega_{p,o}/\Omega_p \tag{56}$$

which is just relaxation determined. We now let $T_{2,p} = T_p$, etc. Then

$$Z_o'' = q\omega_e T_o d_o \frac{(\Omega_p - \Omega_{o,p})/\Omega_p}{1 + T_o^2\,\Delta\omega_o^2 + d_o^2 T_o(\Omega_o\Omega_p - \Omega_{o,p}\Omega_{p,o})/\Omega_p} \tag{57}$$

If we also introduce the generalized no-saturation condition for the observing mode,

$$d_o^2 T_o[(\Omega_o\Omega_p - \Omega_{o,p}\Omega_{p,o})/\Omega_p] \ll 1 \tag{58}$$

one has the simple result that

$$Z_o'' = \frac{T_o q\omega_e d_o}{1 + \Delta\omega_o^2 T_o^2}\left[1 - \frac{\Omega_{o,p}}{\Omega_p}\right] \tag{59}$$

Since Ω_p is always positive,[1] it follows from equation (59) that for $\Omega_{o,p} > 0$, the signal is reduced by the presence of the resonant pump field, while for $\Omega_{o,p} < 0$, the signal is amplified. The limiting (but not realistic) case for equation (59) occurs when W_n is very strong and W_e is negligible. (Here, W_e and W_n are, respectively, the lattice-induced electron spin-flip and nuclear spin-flip rates.) Then the case for the energy levels shown in Figure (2) is easily understood. Let P_i be the population of the ith state. Then saturation by ω_p causes $P_b = P_{b'}$; a strong W_n causes $P_a = P_b$ and $P_{a'} = P_{b'}$, leading to a reduction in intensity of the observed signal. This extreme will be seen to be equivalent to $\Omega_{o,p} = \Omega_o = \Omega_p$.

There are actually two effects that can be seen in ELDOR:

EFFECT 1. The no-saturation effect discussed above is a polarization effect (not unlike an Overhauser effect in NMR), but the two transitions involved have no level in common, and this places special requirements on the relaxation processes in order to obtain significant effects.

EFFECT 2. This effect is important *only* when Z_o'' is being saturated. It reflects the fact that the induced absorption mode Z_p'' acts as an induced transition, which, in conjunction with lattice-induced transitions, can facilitate the rate of energy transferred from the observing radiation field to the lattice via the spin system.

Effect 1 is the main effect in ELDOR, while the analog to Effect 2 is the dominant one in ENDOR. Further details are given in Hyde *et al.*[8] It should, however, be noted that typical ELDOR experiments yield derivative signals for low-enough field-modulation amplitude and frequency.[8] Complicating effects arising from high-enough field-modulation frequency (and amplitude) are discussed in Chapter 5.

3. *ENDOR*

3.1. *General Considerations*

We again consider our four-level system, but now,

$$\begin{aligned}\varepsilon(t) = {} & \tfrac{1}{2}\gamma_e B_e[S_+ \exp(-i\omega_e t) + S_- \exp(+i\omega_e t)] \\ & + \tfrac{1}{2}\gamma_n B_n[I_+ \exp(-i\omega_n t) + I_- \exp(+i\omega_n t)] \\ & + \tfrac{1}{2}\gamma_e B_n[S_+ \exp(-i\omega_n t) + S_- \exp(i\omega_n t)] \\ & + \tfrac{1}{2}\gamma_n B_e[I_+ \exp(-i\omega_e t) + I_- \exp(i\omega_e t)]\end{aligned} \tag{60}$$

In equation (60), the microwave field at frequency ω_e is to induce electron spin flips, while the rf field at frequency ω_n is to induce nuclear spin flips.

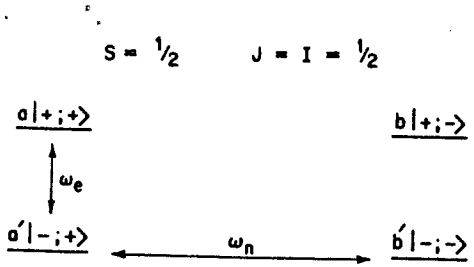

Thus, the last term in equation (60) can be neglected as being too far off resonance to affect the nuclear spins. The third term in equation (60) does have a nontrivial effect on the effective transition moment of the nuclear spins.[6]

This arises from the correction to the high-field wave functions to first order in the off-diagonal hyperfine term: $a_n S_\pm I_\mp$ (e.g., for the four-level system discussed below, the states a' and b are more correctly $(|-+\rangle + \alpha|+-\rangle)$ and $(|+-\rangle - \alpha|-+\rangle)$ where the small mixing coefficient $\alpha = a_n/2B_0$. The effective transition moment is then found to be

$$d_n = d_{n_0}(1 \pm (\gamma_e/\gamma_n)\bar{a}_n/2B_0) \tag{61}$$

where d_{n_0} is the nuclear transition moment in the absence of this correction and the $\pm$ signs correspond to $M_s = \pm)$.

Let us assume the four-level system shown in Figure 3. Let

$$\Delta_e \equiv \omega_e - \omega_{aa'} \approx 0 \tag{62a}$$

$$\Delta_n \equiv \omega_n - \omega_{a'b'} \approx 0 \tag{62b}$$

Then, for assumptions similar to those used for the ELDOR case, we expect important steady-state off-diagonal density matrix elements:

$$\chi_{a'a} = Z_{a'a} e^{i\omega_e t} \equiv Z_e e^{i\omega_e t} \tag{63a}$$

$$\chi_{b'a'} = Z_{b'a'} e^{i\omega_n t} \equiv Z_n e^{i\omega_n t} \tag{63b}$$

We obtain the series of equations:

$$(\Delta_e - i/T_e)Z_e + d_e(\chi_a - \chi_{a'}) + d_n Z_x = q\omega_e d_e \tag{64a}$$

$$(\Delta_n - i/T_n)Z_n + d_n(\chi_{a'} - \chi_{b'}) - d_e Z_x = q\omega_n d_n \tag{64b}$$

$$[\Delta_e + \Delta_n - i/T_x]Z_x - d_e Z_n + d_n Z_e = 0 \tag{64c}$$

where T_e, T_n, and T_x are the T_2 for the ESR, NMR, and cross-transitions, respectively, and all other terms we defined by analogy with previous definitions. Note the appearance of

$$\chi_{b'a} = Z_{b'a}\exp[i(\omega_e + \omega_n)t] \equiv Z_x \exp[i(\omega_e + \omega_n)t] \tag{65}$$

This is an overtone term—a two-quantum effect. Also,

$$\sum_{\alpha \neq a} W_{a\alpha}(\chi_a - \chi_\alpha) = 2d_e Z_e'' \tag{66a}$$

$$\sum_{\alpha \neq a'} W_{a'\alpha}(\chi_{a'} - \chi_\alpha) = -2d_e Z_e'' + 2d_n Z_n'' \tag{66b}$$

$$\sum_{\alpha \neq b} W_{b\alpha}(\chi_b - \chi_\alpha) = 0 \tag{66c}$$

$$\sum_{\alpha \neq b'} W_{b'\alpha}(\chi_{b'} - \chi_\alpha) = -2d_n Z_n'' \tag{66d}$$

Again we may write these equations in the matrix form given by equations (46) with the formal solution given by equations (48) and (49). Note that the **K**, or coherence matrix, is

$$\mathbf{K} = \begin{pmatrix} \Delta_e & 0 & d_n \\ 0 & \Delta_n & -d_e \\ d_n & -d_e & \Delta_e + \Delta_n \end{pmatrix} \tag{67}$$

and is no longer diagonal. Also, intensities are proportional to

$$\mathbf{Q} = q\begin{pmatrix} \omega_e d_e \\ \omega_n d_n \\ 0 \end{pmatrix} \tag{68}$$

but because $\omega_e/\omega_n \sim 660$ for protons, we may usually set

$$\mathbf{Q} \cong q\begin{pmatrix} \omega_e d_e \\ 0 \\ 0 \end{pmatrix} \tag{68'}$$

which amounts to neglecting the analog of Effect 1 in the ENDOR case.

3.2. *Neglect of Coherence Effects*

The coherence effects arise from the off-diagonal elements in the **K** matrix or, in other words, the contribution from Z_x. Consider the case of exact resonance, when $\Delta_e = \Delta_n = 0$, since this is the condition under which

double resonance effects will be maximized. Equations (64)–(66) and (48)–(49) then yield

$$Z_e^{\prime r} = Z_n^{\prime r} = Z_x^{\prime r} = 0 \tag{69a}$$

$$Z_e^{\prime\prime r} = \frac{q\omega_e d_e T_e}{1 + d_e^2(\Omega_e - \xi_e^r)T_e + d_n^2 T_x T_e} \tag{69b}$$

where

$$\xi_e^r = \frac{T_n d_n^2 (T_x + |\Omega_{e,n}|)^2}{1 + d_n^2 \Omega_n T_n + d_e^2 T_x T_n} \tag{69c}$$

Thus, from equation (69b), when

$$1 + d_e^2 \Omega_e T_e \gg d_n^2 T_x T_e \qquad (\text{and } \xi_e^r \not\ll \Omega_e) \tag{70}$$

the coherence effect on $Z_e^{\prime\prime r}$ may be neglected. ξ_e^r leads to an enhancement of a saturated ESR signal, since it effectively reduces the saturation parameter Ω_e. Now, when

$$1 + d_n^2 \Omega_n T_n \gg d_e^2 T_x T_e \tag{71}$$

it follows from (69c) that the ratio ξ_e/Ω_e will not be affected by d_e, and further, if

$$|\Omega_{e,n}| \gg T_x \tag{72}$$

we may completely neglect the coherence effects.

If there is appreciable saturation and

$$d_e^2 \sim d_n^2 \tag{73}$$

then we can replace equations (11)–(13) with the simpler set of conditions

$$\Omega_e,\ \Omega_n,\ |\Omega_{e,n}| \gg T_x \tag{74}$$

for the neglect of coherence effects. The inequalities of equation (74) are fulfilled if the T_1 or saturation parameters are much larger than the T_2 or inverse linewidths.

Now our solutions for Δ_e, $\Delta_n \approx 0$ are

$$Z_e^{\prime\prime} = \frac{q\omega_e d_e T_e}{1 + (\Delta_e T_e)^2 + (\Omega_e - \xi_e)T_e d_e^2} \tag{75a}$$

$$\xi_e = \frac{d_n^2 (\Omega_{e,n})^2 T_n}{1 + (\Delta_n T_n)^2 + d_n^2 T_n \Omega_n} \tag{75b}$$

If the ENDOR spectrum is monitored after subtraction of the ESR signal, then for $\Delta_e = 0$ and $\Omega_e T_e d_e^2 \gg 1$, we have

$$Z_{\text{ENDOR}}^{\prime\prime r} - Z_{\text{ESR}}^{\prime\prime r} = q\omega_e d_e \left(\frac{\Omega_{e,n}^2}{\Omega_e^2}\right) \frac{d_n^2 T_n}{1 + (\Delta_n T_n)^2 + [1 - (\Omega_{e,n}^2/\Omega_e \Omega_n)] T_n \Omega_n d_n^2} \tag{76}$$

Thus, the signal strength is proportional to $(\Omega_{e,n}/\Omega_e)^2$, and the shape is a Lorentzian of width T_n^{-1} and (modified) saturation parameter

$$\Omega_n \left(1 - \frac{\Omega_{e,n}^2}{\Omega_n \Omega_e}\right) \tag{77}$$

The enhancement of an ESR line due to ENDOR is then, from equation (76),

$$E \equiv \frac{Z_{\text{ENDOR}}^{\prime\prime r} - Z_{\text{ESR}}^{\prime\prime r}}{Z_{\text{ENDOR}}^{\prime\prime}} = \frac{\xi_e}{\Omega_e - \xi_e} \xrightarrow[\Delta_n \to 0]{d_n^2 \to \infty} \left(\frac{\Omega_n \Omega_e}{\Omega_{e,n}^2} - 1\right)^{-1} \tag{78}$$

where $d_n^2 \to \infty$ implies

$$d_n^2 T_n \Omega_n \gg 1 \tag{78'}$$

Further details may be found in Ref. 6. Note, however, that typical experimental arrangements yield the derivatives of $Z_{\text{ESR}}^{\prime\prime}$ and $Z_{\text{ENDOR}}^{\prime\prime}$ (see Chapter 2).

3.3. *Coherence Effects in ENDOR*

We now return to equations (62)–(67) and Figure 3. One obtains an **M** matrix [(see equation 49)]:

$$\mathbf{M} = \begin{array}{c} \begin{matrix} \quad e \qquad\qquad\qquad\qquad & \quad n \qquad\qquad\qquad\qquad & \quad x \end{matrix} \\ \begin{pmatrix} 1 + T_e^2\Delta_e^2 + T_e(T_x d_n^2 + \Omega_e d_e^2) & T_e d_e d_n(\Omega_{e,n} - T_x) & T_e d_n[T_e\Delta_e + T_x(\Delta_e + \Delta_n)] \\ T_n d_e d_n(\Omega_{e,n} - T_x) & 1 + T_n^2\Delta_n^2 + T_n(T_x d_e^2 + \Omega_n d_n^2) & -T_n d_e[T_n\Delta_n + T_x(\Delta_e + \Delta_n)] \\ T_x d_n[T_e\Delta_e + T_x(\Delta_e + \Delta_n)] & -T_x d_e[T_n\Delta_n + T_x(\Delta_e + \Delta_n)] & 1 + T_x^2(\Delta_e + \Delta_n)^2 + T_x(T_e d_n^2 + T_n d_e^2) \end{pmatrix} \end{array} \tag{79}$$

Thus we see that the general solution is quite complex, so we consider specific cases[9]:

3.3.1. *Negative ENDOR—Weak Examining ESR Field*

Here we may set all terms in equation (79) containing d_e equal to zero. Let us consider the ENDOR mode of sweeping through ω_n while $\Delta_e = 0$. Then

$$Z_e^{\prime\prime} = q\omega_e d_e T_e \frac{T_x^2\Delta_n^2 + 1 + T_e T_x d_n^2}{T_x^2\Delta_n^2 + (1 + T_e T_x d_n^2)^2} \tag{80}$$

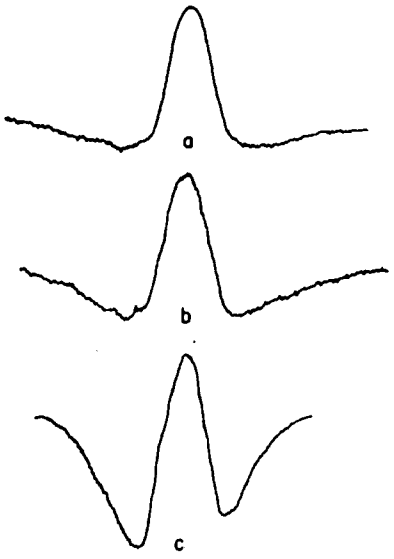

Figure 4. Distorted ENDOR line shapes caused by coherence effects. (a) High B_1^2, long T_{2e}, medium B_n^2. (b) High B_1^2, long T_{2e}, high B_n^2. (c) Low B_1^2, long T_{2e}, high B_n^2.

Thus, a finite d_n acts to reduce the resonant ESR signal, and a maximum reduction occurs for $\Delta_n = 0$. Thus, "negative ENDOR" can be used as a means to detect ENDOR signals.

Now, in order to get appreciable reductions, the quantity $T_e T_x d_n^2$ should not be too much smaller than unity. Usually, $T_x \sim T_e$ (see Ref. 9), so this condition may be restated as "$T_e^2 d_n^2$ should not be too small." Since it is often true that $T_e \ll \Omega_n$, it is not always possible to obtain sufficient rf power to make this method work. An example of negative ENDOR superimposed on a normal ENDOR signal is shown in Figure 4.

The cause of the reduction is readily seen by examining the expression for $\Delta_n = 0$ and ω_e swept. Then

$$Z_e'' = q\omega_e d_e \frac{T_e}{1 + T_e^2\Delta_e^2 + T_e T_x d_n^2(1 - \xi_e)} \tag{81a}$$

with

$$\xi_e = \frac{(T_e + T_x)^2\Delta_e^2}{1 + T_x^2\Delta_e^2 + T_e T_x d_n^2} \tag{81b}$$

The denominator in equation (81a) can have more than one minimum. Thus, differentiating Z_e'' with respect to Δ_e and setting it equal to zero, we get extrema for

$$\Delta_e = 0 \tag{82a}$$

and

$$\Delta_e^2 = yT_x^{-2}[d_n(T_e + T_x)(T_x/T_e)^{1/2} - y] \tag{82b}$$

where

$$y = (1 + T_e T_x d_n^2)^{1/2} \tag{82c}$$

These expressions yield a critical value of d_n

$$d_n^{\text{crit}} = \pm T_x^{-1}(2 + T_x/T_e)^{-1/2} \xrightarrow{T_x \to T_e} \pm 1/\sqrt{3}\,T_e \tag{83}$$

For $d_n > d_n^{\text{crit}}$, there are two peaks in the ESR experiment given by equation (82b), but for $d_n < d_n^{\text{crit}}$, there is only one peak at $\Delta_e = 0$. When $T_e T_x d_n^2 \gg 1$, one has $\Delta_e = \pm d_n$, and it is possible to use this as a method for measuring B_n.

3.3.2. *Very Weak NMR Field*

All terms in equation (79) containing d_n may be set equal to zero. Z_e'' becomes an ordinary saturated Lorentzian and is unaffected by d_n.

3.3.3. *Strong ESR Field but Weaker NMR Field*

Here we require that d_n be still strong enough to saturate the NMR, or

$$T_n\Omega_n d_n^2 \gtrsim 1 \tag{84a}$$

so the induced relaxation effects of the NMR field on the ESR are *not* negligible. We further require that

$$d_e \gg d_n \tag{84b}$$

such that the inequality of equation (70) holds but the inequality of equation (71) is *reversed*. This will lead to a coherence splitting of Z_n'' by d_e, but no splitting of Z_e'' by d_n. The coherence splitting on Z_n'' can then be observed via an ENDOR enhancement technique (see Figure 5), and it could be used to calibrate B_e (or d_e).

3.3.4. *Splitting of ENDOR Lines by a Strong NMR Field*

In this section, we start by assuming that we may neglect the electron–nuclear coherence effects of the type discussed in Sections 3.3.1 to 3.3.3 [i.e., conditions like equations (70) and (71) apply]. The simplest case of interest is then for $S = \frac{1}{2}$, $J = I = 1$ (see Figure 6). There is still a two-quantum transition Z_c involving coherence between the nuclear levels. We thus consider in $\mathbf{Z}$ the four transitions given by Z_e, $Z_\pm \equiv (1/2^{1/2})(Z_1 \pm Z_2)$, and Z_c, where

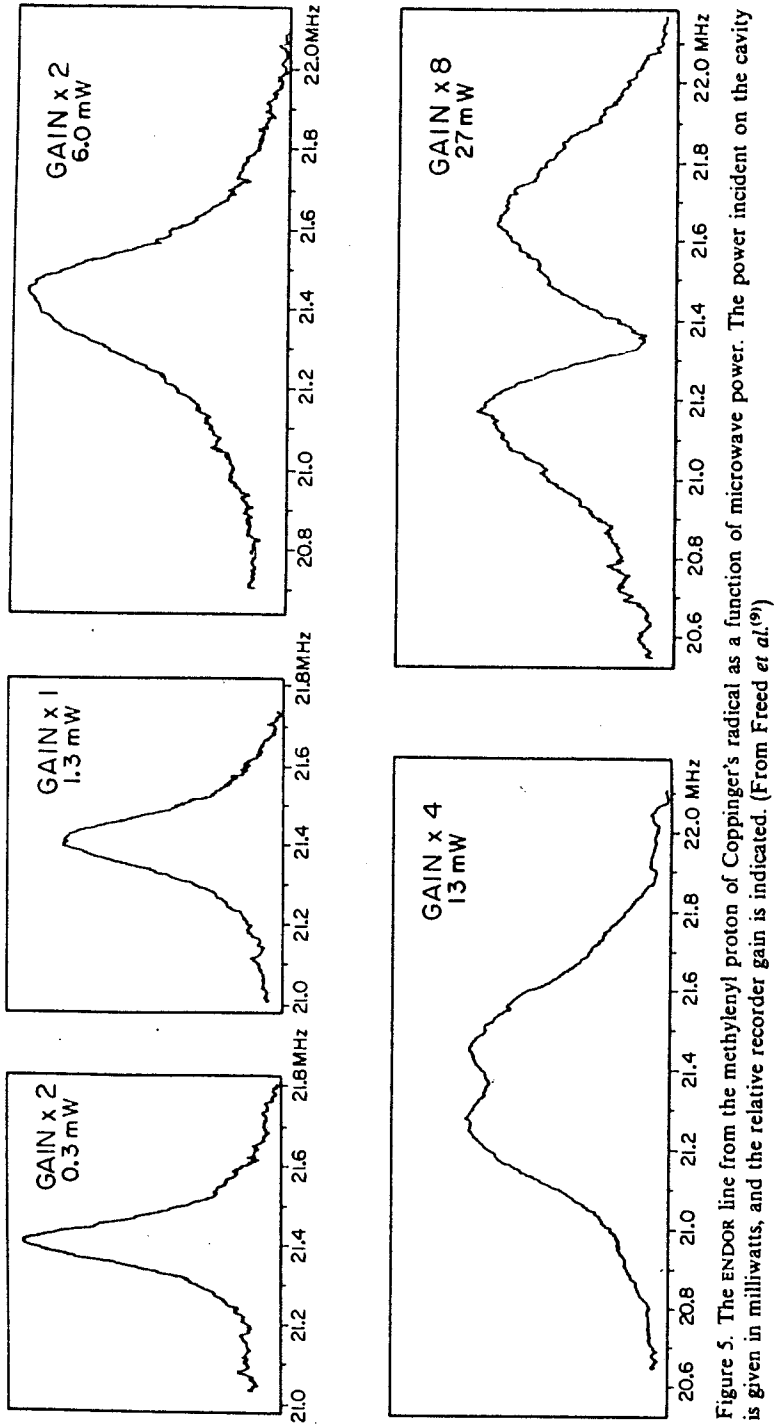

Figure 5. The ENDOR line from the methylenyl proton of Coppinger's radical as a function of microwave power. The power incident on the cavity is given in milliwatts, and the relative recorder gain is indicated. (From Freed *et al.*[9])

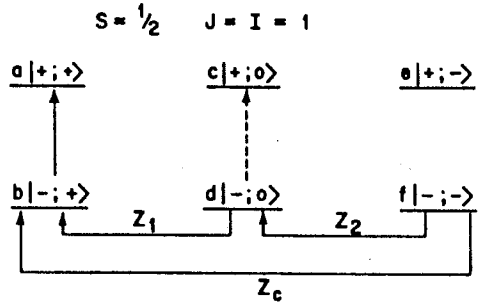

Figure 6. Transitions and eigenstates for double resonance in a radical with $S = \frac{1}{2}$ and a nuclear spin of $I = 1$ (or the $J = 1$ states of two equivalent nuclear spins). (From Freed *et al.*[9])

Z_e can be any of the three allowed ESR transitions in Figure 6. The M matrix in this case is

$$\mathbf{M} = \begin{array}{c} \begin{matrix} e & + & - & c \end{matrix} \\ \begin{pmatrix} 1 + T_e^2\Delta_n^2 + T_e S_{e,+} & (1/\sqrt{2})T_e S_{e,+} & (1/\sqrt{2})T_e S_{e,-} & 0 \\ (1/\sqrt{2})T_+ S_{e,+} & 1 + T_+^2\Delta_n^2 + T_+ S_+ & 0 & 0 \\ (1/\sqrt{2})T_- S_{e,-} & 0 & 1 + T_-^2\Delta_n^2 + T_- S_- + 2d_n^2 T_c T_- & \sqrt{2}(T_- + 2T_c)T_-\Delta_n d_n \\ 0 & 0 & \sqrt{2}\,T_c(T_- + 2T_c)\Delta_n d_n & 1 + 4T_c^2\Delta_n^2 + 2T_c T_- d_n^2 \end{pmatrix} \end{array} \tag{85}$$

where $S_{e,\pm} = S_{e,1} \pm S_{e,2}$ and $T_\pm = T_1 \pm |T_{1,2}|$ [where $T_1 = T_2 = -R_{1,1}(R_{1,1}^2 - R_{1,2}^2)^{-1}$ and $T_{1,2} = -R_{1,2}(R_{1,1}^2 - R_{1,2}^2)^{-1}$ (see Section 4.4.2)].

We see that the symmetric nuclear mode Z_+ does not couple to either Z_- or Z_c, but there is a coherence coupling between Z_- and Z_c. The mode Z''_+ represents the net rf induced absorption from state f to state b. Furthermore, it is easily shown that Z_+ is the only mode that is detected in a conventional NMR experiment, and this is consistent with the well-known result that the only effect of the coherence of the rf field on a simple nuclear resonance experiment appears as a saturation effect with no frequency shifts. The difference mode Z_- is not detected in NMR but does affect the ENDOR spectrum by means of its coupling to Z_e via a finite $S_{e,-}$. Since Z''_- represents the net rf induced absorption from states b and f to state d (i.e., it is proportional to $\sigma_f + \sigma_b - 2\sigma_d$), it does not correspond to any net energy absorption. The coupling of Z_c to Z_- and not Z_+ implies that it does not correspond to any net energy absorption. In fact, when $\Delta_n = 0$, one has $Z''_c = Z'_+ = Z'_- = 0$ and $Z'_c = 2^{1/2} d_n T_c Z''_-$, so at resonance there is only a dispersive mode at the frequency $2\omega_n$.

One may analyze the effects of the coupled nuclear transitions Z_- and Z_c in M given by equation (85) to show that for $T_c \sim T_- \equiv T$, there are extrema for

$$\Delta_n = 0 \quad \text{and} \quad \Delta_n^2 = \tfrac{1}{4}[3d_n(2X)^{1/2} - X] \tag{86}$$

where

$$X = T^{-2}(1 + T^2 d_n^2) \tag{86'}$$

Thus, for $d_n T \gg 1$, we have $\Delta_n = \pm d_n$ or two peaks separated by $2d_n = 2^{1/2}\gamma_n B_n$ (since $J = 1$). Also, there is a critical value $d_n^{\text{crit}} = (4T)^{-1}$ below which there is no splitting but only a single line centered at $\Delta_n = 0$. The effectiveness of the $Z''_\pm$ modes in contributing to ENDOR is determined by the magnitude of the $\Omega_{e,\pm}$. The results depend markedly upon whether the center ESR line or one of the outside ESR lines is saturated, and this may be understood in terms of simple symmetry considerations. We consider the center ESR line first. We note then that $Z''_{db} = Z''_1$ and $Z''_{df} = -Z''_2$ (where a minus corresponds to the transition arrow with a reversed direction) have identical effects on Z''_{0e}; i.e., they enhance symmetrically equivalent paths of relaxation (provided linear M_I-dependent relaxation effects are neglected). Furthermore, the Z''_{0e} transition will have identical Overhauser type of effects on each of these nuclear spin transitions so that $Z''_1 = -Z''_2$ and $Z''_+ = 0$, thereby rendering this mode ineffective in any ENDOR enhancement of Z''_{0e}. [The way this negative relation between Z''_1 and Z''_2 shows up in the detailed analysis is from $\Omega_{0e,1} = -\Omega_{0e,2}$ (see the Appendix).] Therefore only Z''_- can contribute to Z''_{0e}, and it will demonstrate a frequency splitting for large values of d_n. When either of the outside ESR lines is saturated, no such symmetry exists, so both nuclear spin modes may contribute, but in the region of appreciable ENDOR enhancements (i.e., $b \approx 1$), one finds that $\Omega_{\pm e,+} > \Omega_{\pm e,-}$. This means that the relative importance of the Z''_- mode in the ENDOR enhancements is diminished and the coherence effects are much smaller for the outer ESR lines.

This basic treatment and analysis can be generalized to larger J values and to sets of equivalent nuclei. We show in Figure 7 typical computer simulations, demonstrating that the $M = 0$ line does indeed show the dominant effect. This coherence splitting has now been seen in a wide variety of cases. Further aspects of coherence effects are discussed in Ref. 9.

3.4. *Triple Resonance*[10]

We now suppose that the ENDOR experiment is expanded to include a second NMR exciting field that induces the $a \leftrightarrow b$ transition (see Figure 3), yielding a $Z_{ba} \equiv Z_{n'}$ added to equations (63). We shall, for simplicity, neglect

any coherence effects, so that the **K** matrix is diagonal and three dimensional [see equation (8) but now also including $\Delta_{n'} \equiv \omega_{n'} - \omega_{ab} \approx 0$]. In this case the matrix **M** [cf. equation (49)] becomes (see Ref. 10).

$$\mathbf{M} = \begin{pmatrix} 1 + T_e^2\Delta\omega_e^2 + T_e d_e^2\Omega_e & d_e d_n \Omega_{e,n} T_e & d_e d_{n'} \Omega_{e,n'} T_e \\ d_n d_e \Omega_{n,e} T_n & 1 + T_n^2\Delta\omega_n^2 + T_n d_n^2 \Omega_n & d_n d_{n'} \Omega_{n,n'} T_n \\ d_{n'} d_e \Omega_{n',e} T_{n'} & d_{n'} d_n \Omega_{n',n} T_{n'} & 1 + T_{n'}^2 \Delta\omega_{n'}^2 + T_{n'} d_{n'}^2 \Omega_{n'} \end{pmatrix} \tag{87}$$

We again obtain equation (75a) as the solution where now

$$\xi_e = \frac{d_n^2 \Omega_{e,n}^2 T_n (Y_{n'} + d_{n'}^2 T_{n'} \Omega_{n,n'}) + d_{n'}^2 \Omega_{e,n}^2 T_{n'} (Y_n + d_n^2 T_n \Omega_{n,n'})}{Y_n Y_{n'} - d_n^2 d_{n'}^2 \Omega_{n,n'}^2 T_n T_{n'}} \tag{88}$$

and

$$Y_n = 1 + T_n^2 \Delta\omega_n^2 + T_n \Omega_n d_n^2 \tag{89}$$

with an equivalent equation for $Y_{n'}$. Then for $\Delta_n \to 0$ and $d_n^2, d_{n'}^2 \to \infty$ we get

$$\xi_e^r(d_n, d_{n'} \to \infty) = \frac{\Omega_{e,n}^2 (\Omega_{n'} + \Omega_{n,n'}) + \Omega_{e,n'}^2 (\Omega_n + \Omega_{n,n'})}{\Omega_n \Omega_{n'} - \Omega_{n,n'}^2} \tag{90}$$

compared to $\Omega_{e,n}^2/\Omega_n$ for ENDOR. Then the expression for the limiting enhancement [equation (78)] becomes

$$1 + E^{-1} \xrightarrow[\Delta\omega_n \to \infty]{d_n^2 \to \infty} \Omega_e / \xi_e^r(d_n, d_{n'} \to \infty) \tag{91}$$

Note that the limiting conditions on d_n^2 and $d_{n'}^2$ imply not only equation (78'), but also

$$d_n^2 T_n (\Omega_n \Omega_{n'} - \Omega_{n,n'}^2)/\Omega_{n'} \gg 1 \tag{92}$$

as well as the other pair of inequalities resulting from interchanging the indices n and n'. Equation (92) results from the coupled effects of both induced NMR absorptions.

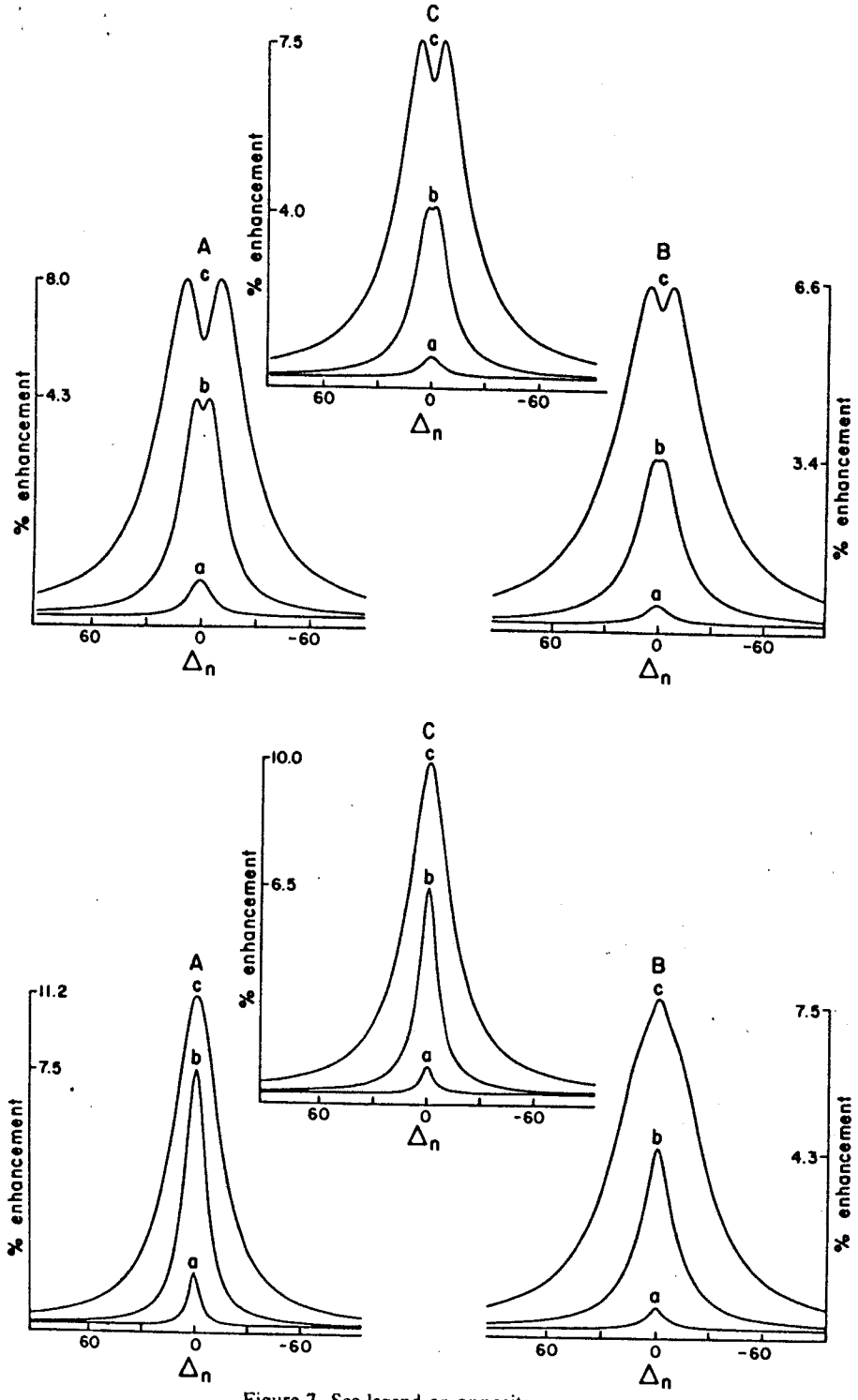

Figure 7. See legend on opposite page.

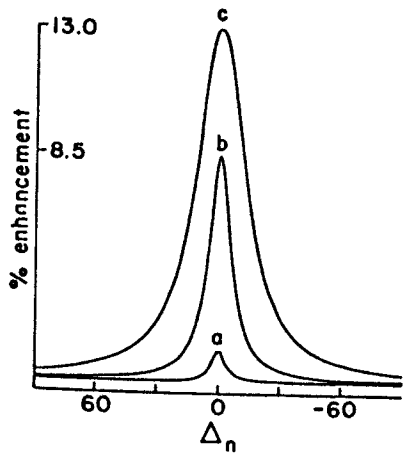

Figure 7. Top, opposite page: ENDOR line shape when the $M_J = 0$ ESR line is saturated, Bottom, opposite page: ENDOR line shape when the $M_J = 1$ ESR line is saturated. To the left: ENDOR line shape when the $M_J = \pm 2$, $J = 2$ ESR line is saturated. (A) $J = 1$, (B) $J = 2$, (C) the composite line from four equivalent spins of $I = \frac{1}{2}$ obtained from A and B properly weighted. All cases correspond to $b = 1$, $T_e^{-1} = 53.3$ units. In A, $d_e = 10.4$; in each, the line shapes a, b, and c correspond to $d_n = 1$, 4, and 10 units, respectively. Each signal height is given relative to the magnitude of the original saturated ESR line. ($W_e = W_n = 1$ frequency unit.) (From Freed *et al.*[9])

4. *Transition Probabilities*

Consider now the general four-level system with all types of spin–lattice relaxation transitions as shown in Figure 8. We can solve for C_{ii} and $C_{ij,kl}$, the cofactors and double cofactors of the W matrix to obtain all the $\Omega_{ij,kl}$.

4.1. *ELDOR—Generalized No-Saturation of Observing Mode*

We have from equation (39) that the signal reduction is given by

$$R \equiv \frac{\%\ \text{reduction}}{100} \tag{93}$$

$$= \frac{\Omega_{o,p}}{\Omega_p} = \frac{W_n^2 - W_{x_1} W_{x_2}}{W_e(2W_n + W_{x_1} + W_{x_2}) + (W_n + W_{x_1})(W_n + W_{x_2})}$$

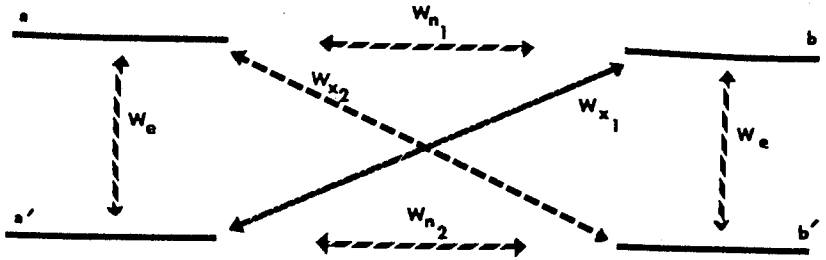

Figure 8. The general four-level system with all types of transitions due to spin–lattice relaxation.

where we have let $W_{n_1} = W_{n_2} = W_n$. Clearly, if $W_n^2 > W_{x_1} W_{x_2}$, one has a reduction in signal, while if $W_n^2 < W_{x_1} W_{x_2}$ there will be an enhancement.

a. Let $W_{x_1} = W_{x_2} = 0$ (i.e., only pseudosecular dipolar terms important). Then

$$R = \frac{W_n}{2W_e + W_n} = \frac{b}{2 + b} \tag{94}$$

where

$$b \equiv \frac{W_n}{W_e} \tag{94'}$$

or a reduction.

b. Let $W_{x_1} = W_n = 0$ (i.e., isotropic hyperfine modulation). Then $R = 0$ (i.e., no effect).

c. Let $W_{x_2} = 4W_n$, $W_{x_1} = \frac{2}{3}W_n$ (dipolar, extreme narrowing). Then

$$R = -\frac{b}{4 + 5b} \tag{95}$$

or an enhancement.

In the case of solids, one can also examine ELDOR enhancements for forbidden ESR transitions.[11] The limiting values for R are given in Table I.

4.2. *ENDOR—Limiting Enhancements*

We have from equation (78) that the enhancement E is given by

$$\begin{aligned} 1 + E^{-1} &= \frac{\Omega_n \Omega_e}{\Omega_{e,n}^2} \\ &= [W_n(2W_e + W_{x_1} + W_{x_2}) + (W_e + W_{x_1})(W_e + W_{x_2})] \\ &\quad \times [W_e(2W_n + W_{x_1} + W_{x_2}) + (W_n + W_{x_1})(W_n + W_{x_2})] \\ &\quad \times [W_{x_2}(W_e + W_n + W_{x_1}) + W_e W_n]^{-2} \end{aligned} \tag{96}$$

a. Let $W_{x_1} = W_{x_2} = 0$ (i.e., only pseudosecular dipolar terms important). Then

$$E = \frac{1}{2[2 + b + b^{-1}]} \begin{cases} \xrightarrow{b \gg 1} \frac{1}{2}b^{-1} \\ \xrightarrow{b \ll 1} \frac{1}{2}b \\ \xrightarrow{b = 1} \frac{1}{8} \end{cases} \tag{97}$$

Table I

ELDOR in the Four-Level System[a,b]

ELDOR experiment (o = observed, p = pumped)	ELDOR enhancement $\equiv -R$ [see equation (93)]	ELDOR frequency (first-order) $\lvert\omega_o - \omega_p\rvert = \Delta P$
p o / o p	$\frac{2(W_{x_1}W_{x_2} - W_{n_1}W_{n_2})}{P}$	a
o p / p o	$\frac{2(W_e^2 - W_{n_1}W_{n_2})}{q}$	$2\omega_n$
p o	$\frac{(W_e + W_{n_1})(W_{x_2} + W_{n_2})(-2)}{P}$	$\lvert\omega_n - \frac{a}{2}\rvert$
o p	$\frac{(W_e + W_{n_2})(W_{x_1} + W_{n_1})(-2)}{P}$	$\lvert\omega_n + \frac{a}{2}\rvert$
p o	$\frac{(W_e + W_{n_2})(W_{x_1} + W_{n_1})(-2)}{P}$	$\lvert\omega_n + \frac{a}{2}\rvert$
o p	$\frac{(W_e + W_{n_1})(W_{x_2} + W_{n_2})(-2)}{P}$	$\lvert\omega_n - \frac{a}{2}\rvert$
o p	$\frac{(W_e + W_{n_1})(W_{x_2} + W_{n_2})(-2)}{q}$	$\lvert\omega_n - \frac{a}{2}\rvert$
p o	$\frac{(W_e + W_{n_2})(W_{x_1} + W_{n_1})(-2)}{q}$	$\lvert\omega_n + \frac{a}{2}\rvert$
o p	$\frac{(W_e + W_{n_2})(W_{x_1} + W_{n_1})(-2)}{q}$	$\lvert\omega_n + \frac{a}{2}\rvert$
p o	$\frac{(W_e + W_{n_1})(W_{x_2} + W_{n_2})(-2)}{q}$	$\lvert\omega_n + \frac{a}{2}\rvert$

[a] From Rist and Freed.[11]

[b] $P = (W_{x_2} + W_{n_2})(2W_e + W_{x_1} + W_{n_1}) + (W_{x_1} + W_{n_1})(2W_e + W_{x_2} + W_{n_2})$;
$q = (W_e + W_{n_1})(W_e + W_{x_1} + W_{x_2} + W_{n_2}) + (W_e + W_{n_2})(W_e + W_{x_1} + W_{x_2} + W_{n_1})$.

b. Let $W_{x_1} = W_n = 0$ (i.e., isotropic hyperfine modulation). Then

$$E = W_{x_2}/W_e \tag{98}$$

This would theoretically be a most effective ENDOR mechanism if W_{x_2} were larger.

c. Case b but now the $a \leftrightarrow b$ ENDOR transition is saturated. Then $E = 0$.

d. Let $W_{x_2} = 4W_n$, $W_{x_1} = \frac{2}{3}W_n$ (dipolar, extreme narrowing).

$$E = \frac{b[22.5 + 60b + 40b^2]}{6 + b[25 + 34b + 15b^2]} \begin{cases} \xrightarrow{b \gg 1} \frac{8}{3}b \\ \xrightarrow{b \ll 1} 3.75b \\ \xrightarrow{b=1} 1.53 \end{cases} \tag{99}$$

This is also a very effective ENDOR mechanism if $b > 1$.

e. Case d but now the $a \leftrightarrow b$ ENDOR transition is saturated

$$E = \frac{b[2.5 + 10b + 10b^2]}{6 + b[45 + 84b + 45b^2]} \begin{cases} \xrightarrow{b \gg 1} \frac{2}{9} \\ \xrightarrow{b \ll 1} \frac{5}{12}b \\ \xrightarrow{b=1} \frac{1}{8} \end{cases} \tag{100}$$

4.3. *Triple Resonance—Limiting Enhancements*

We shall only consider case a, $W_{x_1} = W_{x_2} = 0$. Then one finds

$$E = \frac{W_e}{W_e + W_n} = \frac{1}{1+b} \begin{cases} \xrightarrow{b \gg 1} b^{-1} \\ \xrightarrow{b \ll 1} 1 \\ \xrightarrow{b=1} \frac{1}{2} \end{cases} \tag{101}$$

Thus, for $b \lesssim 1$, one achieves much larger enhancements by triple resonance than by ENDOR, and for $b \ll 1$, one achieves the maximum possible signal enhancement of the saturated ESR of 100%. This is the case where both NMR transitions short out the weak W_n so that the ESR line is being relaxed via its own W_e process and equally well via a W_e process of the other hyperfine line. Thus, triple resonance is potentially a more powerful method than ENDOR.

However, for $b \lesssim 1$ the "effective" saturation of the NMR transitions is determined by satisfying the inequality (92). For the present case, equation (33) becomes

$$4d_n^2 T_n(2W_n + W_e)^{-1} \gg 1 \xrightarrow{b \ll 1} 4d_n^2 T_n/W_e \gg 1 \tag{102}$$

while the simple ENDOR condition of equation (78′) is $d_n^2 T_n/W_n \gg 1$ (for $b \ll 1$), which is much easier to fulfill. Thus, the "effective" saturation of the NMR transitions for the triple resonance experiment can require substantially more rf field strengths than in ENDOR in order to realize its full potential.

4.4. *Expressions for the Linewidths and the Transition Probabilities*

In this section, we consider only the radical concentration-independent contributions to the spin relaxation. We assume a single set of completely equivalent nuclei with total nuclear spin quantum number J and total z component M. [We do not explitly indicate the distinction between degenerate states of the same values of J and M. Note that there will often be degenerate states for a given set of values of J and M. However, it is possible for dipolar terms (but not quadrupolar terms) to order the degenerate states according to a parameter κ or $J^{(\kappa)}$ such that the values of J *and* κ are preserved.[6] We do not explicitly indicate κ in the equations below.] We first consider the transition probabilities.[6]

4.4.1. *Transition Probabilities*

4.4.1.1. *Nuclear Spin Transitions (or Pseudosecular Terms)*

a. Dipolar

$$W_{(M_S, M)\to(M_S, M\pm 1)} = \tfrac{1}{2}j^D(0)[J(J+1) - M(M \pm 1)] \tag{103}$$

where the electron–nuclear dipolar (END) spectral density $j^D(0)$ is

$$j^D(0) = \tfrac{1}{5}\gamma_e^2\gamma_n^2\hbar^2 \sum_m |D^{(m)}|^2 \tau_R \tag{104}$$

with γ_e and γ_n the electronic and nuclear gyromagnetic ratios, respectively, $\hbar = h/2\pi$ with h as Planck's constant, and τ_R is the rotational correlation time, and it is assumed $|\omega_n \tau_R| \ll 1$. The dipolar coefficients are[12]

$$D^{(m)} = \left(\frac{6\pi}{5}\right)^{1/2} \langle \psi_e | r'^{-3} Y_{2,m}(\theta', \phi') | \psi_e \rangle \tag{105}$$

where θ', ϕ', and r' are spherical polar coordinates that define the position of the unpaired electron with respect to a nucleus in the molecular coordinate frame.

b. *Quadrupolar.* (For this case only we consider a single nucleus of spin I):

$$W_{(M_S,\,M)\to(M_S,\,M\pm1)} = 2j^Q(0)[I(I+1) - M(M\pm1)][2M \pm 1]^2 \quad (106a)$$

$$W_{(M_S,\,M)\to(M_S,\,M\pm2)} = 2j^Q(0)[I(I+1) - M(M\pm1)][I(I+1) - (M+1)(M\pm2)] \quad (106b)$$

where

$$j^Q(0) = \frac{\tau_R}{80}\frac{e^2Q^2}{\hbar^2I^2(2I-1)^2}\sum_m |[\nabla\varepsilon]^{(m)}|^2 \quad (107)$$

with electric field gradient irreducible-tensor components[12]:

$$[\nabla\varepsilon]^{(0)} = -(\tfrac{3}{2})^{1/2}\langle\psi_e|V'_{zz}|\psi_e\rangle \quad (108a)$$

$$[\nabla\varepsilon]^{(\pm1)} = \pm\langle\psi_e|V'_{xz} \pm iV'_{yz}|\psi_e\rangle \quad (108b)$$

$$[\nabla\varepsilon]^{(\pm2)} = -\tfrac{1}{2}\langle\psi_e|V'_{xx} - V'_{yy} \pm 2iV'_{xy}|\psi_e\rangle \quad (108c)$$

Also, there will, in general, be cross-terms between the quadrupolar and dipolar interactions.[12]

4.4.1.2. *Electron Spin Transitions (or Nonsecular Terms)*

$$W_{(\mp,\,M)\to(\pm,\,M)} = 2j^D(0)M^2 + 4j^{(DG2)}(\omega_o)B_oM + 2j^{(G2)}(\omega_o)B_o^2 + W_e^{SR} \quad (109)$$

Here

$$j^D(\omega_o) = j^D(0)[1 + \omega_o^2\tau_R^2]^{-1} \quad (110)$$

The g-tensor spectral density is

$$j^{(G2)}(\omega_o) = \frac{1}{20}\beta_e^2\hbar^{-2}\left\{\sum_{k=1}^{3}(g_k)^2 - 3g_s^2\right\}\frac{\tau_R}{1+\omega_o^2\tau_R^2} \quad (111)$$

where β_e is the Bohr magneton. The g-tensor dipolar cross-term spectral density is

$$j^{(DG2)}(\omega_0) = -\frac{1}{10}\gamma_e\beta_e\gamma_n\sum_m D^{(m)}g^{(m)}\frac{\tau_R}{1+\omega_0^2\tau_R^2} \quad (112)$$

with $g^{(0)} = 6^{-1/2}[2g'_z - (g'_x + g'_y)]$ and $g^{(\pm2)} = \frac{1}{2}(g'_x - g'_y)$. The spin rotational contribution to W_e is in a semiclassic treatment:

$$W_e^{SR} = \frac{IkTC^2}{\hbar^2}\left(\frac{\tau_J}{1+\omega_0^2\tau_J^2}\right) \quad (113)$$

where I is the moment of inertia, C is the spin rotational constant of the radical (and we have assumed both to be isotropic), and τ_J is the correlation time for the angular momentum.[13] In liquids, usually $\tau_J \ll \tau_R, \omega_0^{-1}$. One has for a Stokes–Einstein model

$$\tau_R = 4\pi\eta a^3/3kT \quad (114a)$$

$$\tau_J = [6IkT\tau_R]^{-1} \quad (114b)$$

More generally[13] $\mathbf{C} \cong -2\mathbf{A}\,\Delta\mathbf{g}$ where $\mathbf{A}$ is the inverse moment-of-inertia tensor and $\Delta\mathbf{g} = \mathbf{g} - 2.00231$. Then we have (for axially symmetric $\mathbf{A}$):

$$W_e^G \cong \sum_i (g_i - g_s)^2/40\tau_R \qquad \text{for } \omega_o^2\tau_R^2 \gg 1 \quad (115a)$$

$$W_e^{SR} \cong \sum_i (g_i - g_e)^2/18\tau_R \quad (115b)$$

If these are the dominant terms in W_e, then (see Ref. 7):

$$W_e \propto \tau_R^{-1} \quad (116a)$$

or

$$W_e \equiv AT/\eta \quad (116b)$$

Usually, $\tau_R > \omega_0^{-1}$ for free radicals in liquids below room temperature, since at X band $\omega_0^{-1} \cong 1.7 \times 10^{-11}$ sec. Then pseudosecular dipolar terms dominate in ELDOR or ENDOR. So, from equations (103) and (104),

$$W_n \propto \tau_R$$

or

$$W_n \equiv B\eta/T$$

Then

$$b = \left(\frac{B}{A}\right)\left(\frac{\eta}{T}\right)^2 \quad (117)$$

If we let

$$\eta \propto Te^{W/kT}, \qquad W > 0$$

we get b increasing significantly with decreasing T. This usually leads to better ELDOR and ENDOR signals at reduced temperatures.

The typical linear dependence of W_e on T/η, as well as the dependence of the linewidth parameters (from which W_n is determined) on η/T are shown in Figures 9 and 10.

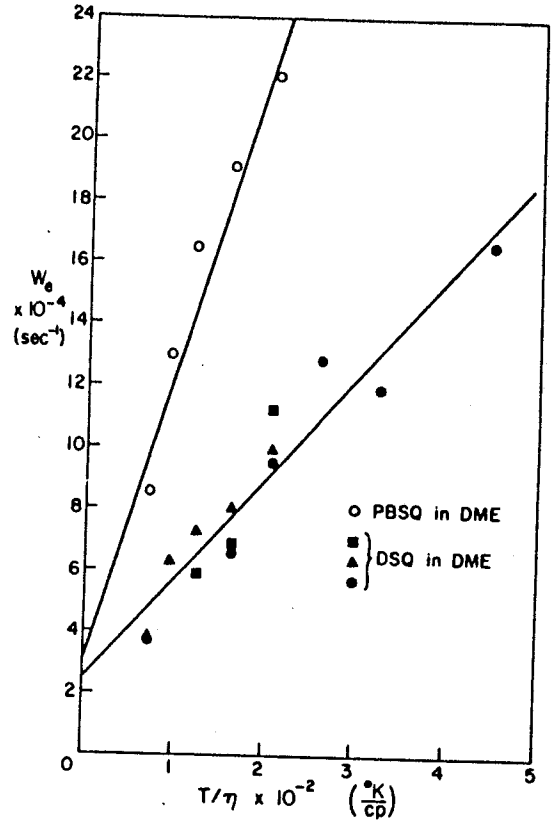

Figure 9. W_e as a function of T/η for solutions of PBSQ and DSQ in DME.

4.4.1.3. *Combined Electron Spin–Nuclear Spin Transitions (Cross-Relaxation from Nonsecular Terms)*

$$W_{M_s, M \to M_s \pm 1, M \mp 1} = [\tfrac{1}{3}j^{(D)}(\omega_0) + \tfrac{1}{2}j^{I}(\omega_0)][J(J+1) - M(M \mp 1)] \quad (118)$$

$$W_{M_s, M \to M_s \pm 1, M \pm 1} = 2j^{(D)}(\omega_0)[J(J+1) - M(M \pm 1)] \quad (119)$$

The isotropic dipolar spectral density is

$$j^{I}(\omega) = \tfrac{1}{2}\gamma_e^2 \int_{-\infty}^{-\infty} [\langle a(t)a(t+\tau)\rangle - \bar{a}^2]e^{-i\omega\tau}\, d\tau \quad (120)$$

where $\bar{a}$ is the time-averaged hyperfine splitting. Note that for $j^{D}(\omega_0) \ll j^{D}(0)$ [and small $j^{I}(\omega_0)$], $W_x \ll W_n$ and pseudosecular terms dominate as noted above.

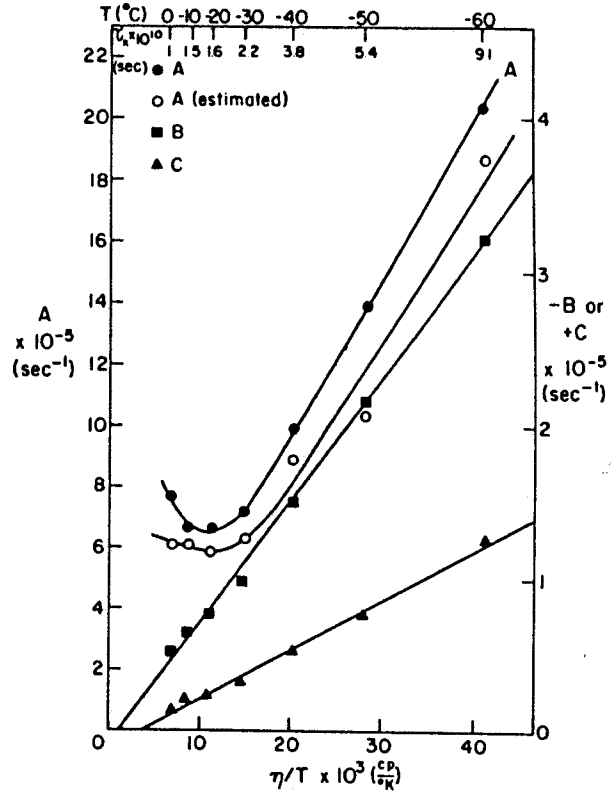

Figure 10. The ESR linewidth parameters A, B, and C for a dilute solution of PBSQ in ethanol as a function of η/T. W_n is usually determined from C.

4.4.2. *Linewidths*

One finds in the analysis of the relaxation matrix for the diagonal elements $R_{ab,ab}$ yielding the linewidths, that[1,2,6,12]

$$T_{2a,b}^{-1} = -\mathrm{Re}\, R_{ab,ab} = T_{2a,b}^{-1} + \tfrac{1}{2}\left(\sum_{\gamma \neq a} W_{a\gamma} + \sum_{\gamma \neq b} W_{b\gamma}\right) \quad (121)$$

where

$$T_{2a,b}^{-1} = \int_0^{\infty} \langle \omega^{a,b}(t)\omega^{a,b}(t-\tau)\rangle\, d\tau \quad (122)$$

and

$$\omega^{a,b}(t) \equiv [\mathscr{H}_1(t)_{aa} - \langle \mathscr{H}_1(t)\rangle_{aa}] - [\mathscr{H}_1(t)_{bb} - \langle \mathscr{H}_1(t)\rangle_{bb}] \quad (123)$$

In equations (122) and (123), the angular brackets imply an ensemble average over the randomly fluctuating spin perturbation term $\mathcal{H}_1(t)$. The term $T_{2a,b}^{-1}$ is seen to result from fluctuations in the eigenenergy difference between the two states a and b, which depends only on the diagonal elements of the perturbation $\mathcal{H}_1(t)$, so this contribution is known as the secular contribution to the linewidth. The terms in equation (131) of type $W_{a\gamma}W_{b\gamma}$ give the mean of all the transitions away from states a and b. These are the nonsecular (as well as pseudosecular) terms yielding line broadening due to the Heisenberg uncertainty in lifetime effect. We also note that the imaginary parts of $R_{ab,ab}$ are not, in general, zero. One sees, from the form of equations (5), that these imaginary terms must cause frequency shifts and are therefore called "dynamic frequency shifts." They are of potential importance, but partly because they are not often studied, we will not discuss them further here. Their contributions in simple cases have been reviewed by Fraenkel.[14] We give below the expressions for the $T_{2a,b}^{-1}$.[6,12]

a. States a and b involve an electron spin–flip transition.

$$\begin{aligned} T_{2a,b}^{-1} = {} & (1/4)[j^{(1)}(0) + (8/3)j^{(D)}(0)](M_a + M_b)^2 \\ & + [j^{(1G0)}(0) + (8/3)j^{(DG2)}(0)]B_0(M_a + M_b) \\ & + [j^{(G0)}(0) + (8/3)j^{(G2)}(0)]B_0^2 \end{aligned} \tag{124}$$

The new spectral density terms here are

$$j^{(G0)}(0) = \beta_e^2\hbar^{-2}\tfrac{1}{2}\int_{-\infty}^{\infty}[\langle g_s(t)g_s(t+\tau)\rangle - \bar{g}_s^2]e^{-i\omega\tau}\,d\tau \tag{125}$$

where $\bar{g}_s$ is the time-averaged g value and

$$j^{(1G0)}(0) = \tfrac{1}{2}\bar{g}_s\beta_e^2\hbar^{-2}\int_{-\infty}^{\infty}[\langle a(t)g_s(t+\tau)\rangle - \bar{a}\bar{g}_s]\,d\tau \tag{126}$$

Also, M_a and M_b are the z-component quantum numbers of the equivalent set of nuclear spins in states a and b, respectively. Note that an allowed ESR transition corresponds to $M_a = M_b$, while $M_a \neq M_b$ is a forbidden ESR transition.

b. Linewidths for nuclear transitions (i.e., $\Delta M_s = 0$).

$$T_{2a,b}^{-1} = (1/4)[j^{(1)}(0) + (8/3)j^{(D)}(0)][M_a - M_b]^2 \tag{127}$$

When $M_a - M_b = \pm 1$, we have a single-quantum NMR transition, while for $M_a - M_b = \pm n$, we have an n-tuple quantum NMR transition. The pseudosecular and nonsecular contributions to $T_{2a,b}^{-1}$ are obtained with the use of equation (121). However, there are also off-diagonal R-matrix elements that

must be included for the nuclear transitions. They may be written as

$$-R^{\text{pseudosec}}_{M,M+1;M+1,M+2} = -\tfrac{1}{2}j^{(D)}(0)[f(J,-M)f(J,-(M+1))] \tag{128}$$

and

$$-R^{\text{pseudosec}}_{M-1,M;M,M+1} = -\tfrac{1}{2}j^{(D)}(0)[f(J,M)f(J,(M+1))] \tag{129}$$

where

$$f(J,\pm M) \equiv [(J \pm M)(J \mp M + 1)]^{1/2} \tag{130}$$

The subscripts on R indicate the values of M_J of the states being coupled. The quadrupolar terms will also make secular contributions as well as off-diagonal contributions to the matrix **B** for the nuclear transitions. Aspects of such terms are discussed elsewhere.[12]

In concluding this section, we note that more detailed analyses of these spectral densities in terms of realistic models both for isotropic as well as ordered fluids appear in several places.[12–23]

5. *Heisenberg Spin Exchange and Chemical Exchange*

Heisenberg spin exchange is a very important radical-concentration-dependent relaxation mechanism in normal liquids. It is probably the dominant one for $S = \frac{1}{2}$. It may be analyzed by a simple model, which also serves as a simple example of the stochastic Liouville approach (see Section 8). We assume radicals exist either as well-separated "monomers" or as interacting pairs or "dimers," each with mean lifetimes τ_2 and τ_1, respectively, and with density matrices σ and ρ, respectively. The equations of motion are then:

$$i\dot{\sigma} = \mathcal{H}_0^{(1)x}\sigma + i\frac{2}{\tau_2}\text{Tr}_s\rho - i\frac{2}{\tau_2}\sigma \tag{131}$$

$$i\dot{\rho} = (\mathcal{H}_0^{(1)x} + \mathcal{H}_0^{(2)x} + \mathcal{H}_J^{x})\rho - i\tau_1^{-1}(\rho - \sigma\times\sigma) \tag{132}$$

where $\mathcal{H}_0^{(1)}$ is the spin Hamiltonian for radical 1, etc., and $\text{Tr}_s\rho = \frac{1}{2}(\text{Tr}_1\rho + \text{Tr}_2\rho)$ is a symmetrized trace over each of the two components of the interacting dimer, and we have used the superoperator form, e.g., $\mathcal{H}_0^{x}\sigma = [\mathcal{H}_0, \sigma]$. Also,

$$\mathcal{H}_J = JS^{(1)}\cdot S^{(2)} \tag{133}$$

where J is twice the exchange integral. One obtains a steady-state solution for σ in the rotating frame. It is then possible to show that when

$$|J|, \tau_1^{-1} \gg |a_i|, \gamma_e B_1 \tag{134}$$

Equation (131) is well approximated by

$$i\dot{\sigma} = \mathscr{H}_0^{(1)x}\sigma + i\omega_{HE}[\mathrm{Tr}_s(\mathscr{P}\sigma \times \sigma\mathscr{P}) - \rho] \tag{135}$$

where

$$\omega_{HE} = \frac{1}{\tau_2}\frac{J^2\tau_1^2}{1 + J^2\tau_1^2} \tag{136}$$

is the Heisenberg exchange frequency. In equation (135), we have neglected a frequency shift term that is readily shown to be zero in the high-temperature approximation [i.e., $A\sigma \cong 1 + \sigma'$ with $|\sigma'| \ll 1$] (see equation 24). Here, $\mathscr{P}$ is the operator that permutes electron spins. The derivation of equation (135) is based on the fact that for spins $S = \frac{1}{2}$,

$$\mathscr{H}_J^x = \tfrac{1}{2}J\mathscr{P}^x \tag{137}$$

For simple Brownian diffusion of the radicals in solution, we have

$$\tau_2^{-1} = 4\pi D f \mathscr{N} \tag{138a}$$

$$\tau_1^{-1} = (6D/d^2) f e^u \tag{138b}$$

where $\mathscr{N}$ is the density of radicals, the diffusion coefficient is $D = kT/6\pi a\eta$, and d is the interaction distance for exchange. The factors f and fe^u are introduced for charged radicals to take account of Coulombic and ionic atmosphere effects.[24,25]

The result, equation (135), means that Heisenberg exchange appears as a simple exchange process analogous to chemical exchange processes for which the well-known Kaplan–Alexander[26] method applies. We let

$$\Phi_H(\chi) \equiv \omega_{HE}[\mathrm{Tr}_s(\mathscr{P}\sigma \times \sigma\mathscr{P}) - \sigma] \tag{139}$$

and add this relaxation term to equation (5). One then finds that for well-separated hyperfine lines, the T_2 contributions are

$$T_{2,HE}^{-1}(\mathrm{ESR}, \lambda) = \left(\frac{A - 2D(\lambda)}{A}\right)\omega_{HE} \tag{140}$$

$$T_{2,HE}^{-1}(\mathrm{NMR}) = \tfrac{1}{2}\omega_{HE} \tag{141}$$

Here $D(\lambda)$ is the degeneracy of the λth transition, and the $T_2^{-1}(\mathrm{NMR})$ is the width contribution to a well-resolved ENDOR line. The diagonal elements of equation (139) yield

$$[\Phi_H(\chi)]_{\alpha\pm\alpha\pm} = \tfrac{1}{2}\omega_{HE}[(\chi_{\alpha\mp} - \chi_{\alpha\pm}) \pm (\chi_+ - \chi_-)]$$

$$= \mp\frac{\omega_{HE}}{2}\left[\left(1 - \frac{2}{A}\right)\hat{\chi}_\alpha - \sum_{\gamma\neq\alpha}\frac{2}{A}\hat{\chi}_\gamma\right] \tag{142}$$

where

$$\chi_\pm = \frac{2}{A}\sum_\gamma \chi_{\gamma\pm} \tag{143a}$$

and

$$\chi_+ + \chi_- = 0 \tag{143b}$$

and

$$\hat{\chi}_\alpha \equiv \chi_{\alpha+} - \chi_{\alpha-} \tag{143c}$$

The notation $\alpha\pm$ in equations (142) and (143) refers to the αth nuclear spin configuration, and $M_s = \pm$.

The steady-state solution of equation (142) in equation (5) is

$$\chi_{\alpha+} - \chi_{\alpha-} = 2\chi_+ \tag{144}$$

i.e., differences in population between all pairs of levels differing only in M_s are equal. The unlinearized rate equations yield the steady-state result that all the ratios $\sigma_{\alpha-}/\sigma_{\alpha+}$ are equal.

If in chemical exchange (CE) (i.e., electron transfer), the predominant NMR relaxation of the diamagnetic radical precursors is the CE process, then CE appears to be just like HE in magnetic resonance experiments on the radicals and we indicate this by replacing ω_{HE} by the more general symbol ω_{EX} (see Ref. 7 for further details).

We now consider the W matrix including equation (142). Note first that equation (142) generates a matrix $\mathbf{W}^{HE}$, which is symmetric and which has the properties that the sums of all columns (rows) are all zero. Thus, all the theorems of the Appendix apply to the complete W matrix, including equation (142). Now, however, note that

$$[\Phi_{HE}(\chi)]_{\alpha+\alpha+} + [\Phi_{HE}(\chi)]_{\alpha-\alpha-} = 0 \tag{145}$$

so each pair of rows of W labeled $\alpha+$ and $\alpha-$ are linearly dependent. Thus, while $\mathbf{W}^{HE}$ is an $A \times A$ matrix, it is of rank $A/2$; i.e., HE does not act to change $(\chi_{\alpha+} + \chi_{\alpha-})$ but rather to equate all $(\chi_{\alpha+} - \chi_{\alpha-})$. One must add W_n or W_x terms to reduce this high-order singularity.

One may alternatively employ another method. Sufficient conditions for this method are:

Condition 1. All spin-flip relaxation transitions are of W_e, W_n, or ω_{HE} type (i.e., no W_x).

Condition 2

(a) $W_{(+,M)\to(-,M)} = W_{(-,M)\to(+,M)}$ (146a)

(b) $W_{(+,M)\to(+,M\pm1)} = W_{(-,M)\to(-,M\pm1)}$ (146b)

Then we may define a $\frac{1}{2}A$-dimensional square matrix $\hat{\mathbf{W}}$ (which is usually nonsingular or readily separated into nonsingular components) according to

$$[\hat{\mathbf{W}}\hat{\chi}]_\lambda \equiv [\mathbf{W}\chi]_{\lambda+} - [\mathbf{W}\chi]_{\lambda-} \tag{147}$$

This reduced eigenstate space is found to include only the $\hat{\chi}_\lambda \equiv \chi_{\lambda+} - \chi_{\lambda-}$, which are closely related to pure ESR transitions.

Then, if only ESR transitions are induced, we find

$$S_{\lambda,\eta} = 4d_\lambda d_\eta(\hat{\mathbf{W}}^{-1})_{\lambda,\eta} = d_\lambda d_\eta \Omega_{\lambda,\eta} \tag{148}$$

[This method can also be generalized for ENDOR (see Section 6.2).] Using this method, one can then prove[24]

$$\Omega_\lambda = \frac{2}{W_e D(\lambda)} \frac{1 + D(\lambda)b''}{1 + \frac{1}{2}Ab''} \tag{149}$$

$$b'' = \omega_{\text{HE}}/AW_e \tag{149'}$$

with

$$T_{1,\lambda} = \tfrac{1}{4}[D(\lambda)\Omega_\lambda] \tag{150}$$

and

$$\Omega_{\lambda,\eta} = \frac{2}{W_e} \frac{b''}{1 + \frac{1}{2}Ab''} \lambda \neq \eta \tag{151}$$

Equation (149) illustrates the "shorting-out" effect spin exchange has in coupling the different hyperfine lines [see equation (144)] without directly leading to electron spin-flips. It follows from equations (54) and (149)–(151) that

$$R \equiv \frac{Z''_{\text{ESR}} - Z''_{\text{ELDOR}}}{Z''_{\text{ESR}}} \tag{152}$$

is [for $\Delta\omega_0 = 0$ and the no-saturation condition of equation (58)]

$$R^{-1} = \Omega_p/\Omega_{o,p} + [(1 + \Delta\omega_p^2 T_p^2)/T_p\Omega_{o,p}]\, dp^{-2} \tag{153}$$

and

$$R_\infty^{-1} = \Omega_p/\Omega_{o,p} = \frac{1 + D(p)b''}{D(p)b''} = [D(p)b'']^{-1} + 1 \tag{154}$$

Here, R_∞ is defined in the same manner as the asymptotic R of equation (93). Equation (154) shows how Heisenberg spin exchange is effective in enabling significant ELDOR reduction factors. Equation (154) has been confirmed experimentally, as shown in Figure 11.

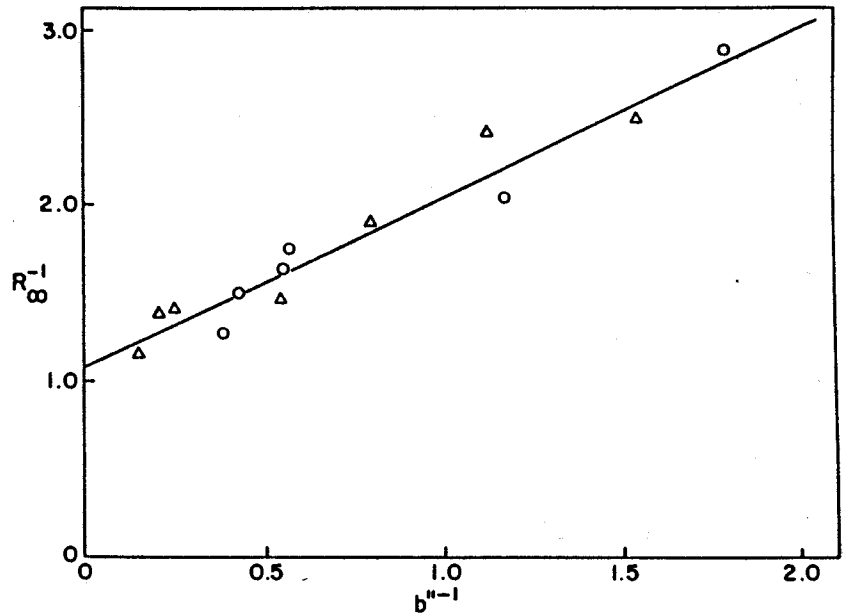

Figure 11. Linear least-squares fit for R_∞^{-1} versus b''^{-1} for aqueous PADS solutions at 24°C; Δ = data for two hyperfine line separation ($\tilde{M} = 1$ line observed and $\tilde{M} = -1$ line pumped); O = data for one hyperfine line separation ($M = 0$ line observed and $M = -1$ line pumped). The slope and intercept are 1.03 ± 0.08 and 1.07 ± 0.07, respectively, as compared to values of unity theoretically predicted. (From Eastman *et al.*[251])

Now for ENDOR and a single nucleus of spin $I = \frac{1}{2}$ with $W_x = 0$, one has

$$\Omega_e = \frac{1}{W_e} \frac{[2W_e + (W_n + \omega_{\text{HE}}/2)]}{W_e + (W_n + \omega_{\text{HE}}/2)} \tag{155a}$$

$$\Omega_n = \frac{1}{W_n} \frac{[2W_n + (W_e + \omega_{\text{HE}}/2)]}{[W_e + \omega_{\text{HE}}/2 + W_n]} \tag{155b}$$

$$\Omega_{e,n} = (W_e + W_n + \omega_{\text{HE}}/2)^{-1} \tag{155c}$$

and

$$\xi_e^r(d_n \to \infty) = \frac{W_n}{(2W_n + W_e + \omega_{\text{HE}}/2)(W_e + W_n + \omega_{\text{HE}}/2)} \tag{156}$$

In general, if $W_n = 0$ and $W_x = 0$, then $\xi_e^r(d_n \to \infty) = 0$ even for more than one magnetic nucleus. Thus Heisenberg exchange is *not* an effective ENDOR mechanism; i.e., it is ENDOR "inactive," although it is ELDOR "active." The manner in which Heisenberg exchange suppresses ENDOR enhancements is

illustrated in Figure 12 representing a concentration-dependent study, while the T/η dependence of the exchange contribution to the ENDOR linewidths as predicted by equations (141), (136), and (138a) for strong exchange are illustrated in Figure 13.

In the case of triple resonance, one has

$$\Omega_{n,n'} = \frac{1}{W_n}\frac{W_e + \omega_{HE}/2}{W_e + W_n + \omega_{HE}/2} \tag{157}$$

$$\xi_e^r(d_n, d_{n'} \to \infty) = \frac{1}{W_e + W_n + \omega_{HE}/2} \tag{158}$$

and

$$E = \frac{W_e}{W_e + W_n + \omega_{HE}/2} \tag{159}$$

so that maximum enhancements accrue from $W_e \gg W_n, \omega_{HE}$.

More detailed models of Heisenberg spin exchange are summarized elsewhere.[27,28] Also, another concentration-dependent relaxation mechanism, which can become important at reduced temperatures, is that of intermolecular dipolar interactions between electron spins. Its ENDOR effects are discussed in some detail by Leniart *et al.*[29]

In concluding the last two sections, we note that the characteristic behavior of the various relaxation mechanisms as differently manifested in linewidth, saturation, ENDOR, and ELDOR is a useful approach for separating out the many possible components of relaxation in a particular paramagnetic system. We present in Table 2 a simplified summary of these characteristics.

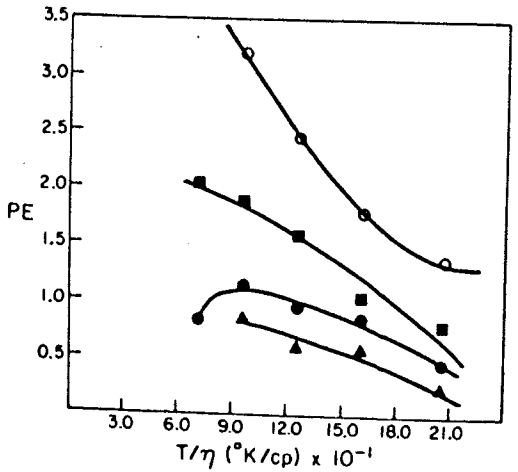

Figure 12. The percent enhancement at infinite rf power as a function of T/η for solutions of DSQ in DME; ▲ = concentration of 9.9×10^{-4} M; ● = concentration of 6.3×10^{-4} M; ■ = concentration of 3.0×10^{-4} M; ○ = concentration of 1.5×10^{-4} M.

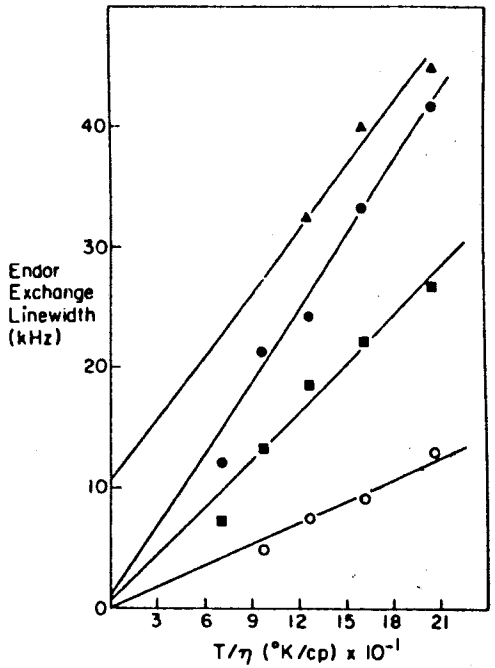

Figure 13. The exchange contribution to the ENDOR linewidth as a function of T/η for solutions of DSQ in DME. ▲ = 9.9×10^{-4} M; ● = 6.3×10^{-4} M; ■ = 3.0×10^{-4} M; ○ = 1.5×10^{-4} M.

6. *General Approach*

One finds that, in general, multiple resonance ESR experiments in liquids may be expressed in the matrix form equation (46) with formal solution given by equations (48)–(51).[6] In this formal solution, **Z** is a vector in the space of all induced transitions and **X** is a vector in the space of all spin eigenstates. The only requirement is that a *raising* convention apply. This is the requirement that all induced transitions in the space of **Z** are those in which there is (are) increase(s) in spin quantum number but *no* decrease(s) in spin quantum number (see Ref. 9). This requirement is often met for ENDOR and ELDOR experiments, but it sometimes requires neglect of some multiple quantum transitions. If it is not met, then a somewhat more complex form of equations (40) and (48)–(51) could become necessary. Also, in summary, the validity of the general relaxation equation (15) for well-separated hyperfine lines requires that

$$|\gamma_e B_0|, |\gamma_i B_0|, |\gamma_e \bar{a}_i|, \tau_c^{-1} \gg \varepsilon(t), |R| \tag{160}$$

where τ_c refers to the relevant correlation time(s). We outline below a "diagram method" for constructing the matrices needed for equations (46) and (48)–(51).

Table 2. ESR Linewidth and Relaxation Mechanisms

Mechanism	Linewidths: Nuclear spin dependence	Linewidths: Field frequency dependence	Linewidths: Temperature and viscosity	Saturation (Ω): Activity	Saturation (Ω): Nuclear spin dependence	ELDOR: Activity	ENDOR: Activity	ENDOR: Linewidth contribution	ENDOR: Enhancement (%) (maximum)
Intramolecular									
G-Isotropic—secular only	None	Quadratic	As τ_c	None	None	None	None	None	None
Dipole-isotropic									
Secular	M^2	None	As τ_c	None	—	None	None	Yes	—
Nonsecular	M^2	$[1+\omega_0^2\tau_c^2]^{-1}$	As $\tau_c[1+\omega_0^2\tau_c^2]^{-1}$	W_{x_1}	Yes	None unless $W_{x_2}\neq 0$	W_{x_1}	Yes	Goes as W_{x_1}/W_e
Isotropic *G*-dipole									
X-Term—secular only	M	Linear	As τ_c	None	—	None	None	None	—
G-Anisotropic									
Secular	None	Quadratic	$\tau_R \propto \eta/T$	None	—	None	None	None	—
Nonsecular	None	$\omega_0^2[1+\omega_0^2\tau_R^2]^{-1}$	$\tau_R[1+\omega_0^2\tau_R^2]^{-1}$	W_e	None	W_e	W_e	Yes	W_e
Dipole-anisotropic									
Secular ($S_z I_z$)	M^2	None	τ_R	None	—	None	None	Yes	—
Pseudosecular ($S_z I_\pm$)	M^2	None	τ_R	W_a	Yes	W_a reduction	W_a	Yes	$W_a/W_e \sim 1$
Nonsecular									
$S_\pm I_z$	M^2	$[1+\omega_0^2\tau_R^2]^{-1}$	$\tau_R[1+\omega_0^2\tau_R^2]^{-1}$	W_e	M^2	W_e	W_e	Yes	W_e
$S_\pm I_\pm$, $S_\pm I_\mp$	M^2	$[1+\omega_0^2\tau_R^2]^{-1}$	$\tau_R[1+\omega_0^2\tau_R^2]^{-1}$	W_{x_1}, W_{x_2}	Yes	W_x enhancement	W_{x_1}, W_{x_2}	Yes	Goes as W_x/W_e
Anisotropic *G*-dipole *X*-term									
Secular	M	Linear	τ_R	None	—	None	None	None	None
Nonsecular	M	$\omega_0[1+\omega_0^2\tau_R^2]^{-1}$	$\tau_R[1+\omega_0^2\tau_R^2]^{-1}$	W_e	M	W_e	W_e	Yes	W_e
Quadrupolar									
Secular	No width contribution M^2 and M^4	—	τ_R	None	—	None	None	Yes	—
Pseudosecular		None	τ_R	W_a	Yes	W_a reduction	W_a	Yes	$W_a/W_e \sim 1$
Spin rotation									
Secular	None	None	$\tau_J \propto T/\eta$	None	—	None	None	None	—
Nonsecular	None	None	$\tau_J \propto T/\eta$	W_e	None	W_e	W_e	Yes	W_e
Intramolecular spin–orbit processes									
Secular	None	None	Independent	None	—	None	None	None	—
Nonsecular	None	None	Independent	W_e	None	W_e	W_e	W_e	W_e
Zero-field splitting $S > \frac{1}{2}$									
Secular	None	None	τ_R	None	—	None	None	None	—
Nonsecular	None	$[1+b^2\omega_0^2\tau_R^2]^{-1}$	$\tau_R[1+b^2\omega_0^2\tau_R^2]^{-1}$	W_e type	None	W_e type	W_e type	Yes	W_e type
Intermolecular									
Heisenberg spin exchange (+electron transfer)	Symmetric dependence on D_M	None	$T/\eta[1+(J\tau_1)^{-2}]^{-1}$ $\tau_1 \propto \eta/T$ for HE	ω_{EX}	Some dependence on D_M	ω_{EX} reduction	No	Yes	Decreases enhancements
Dipole–Dipole									
Secular									
$S_{1z}S_{2z} + S_{1\pm}S_{2\mp}$ like	Symmetric dependence on D_M	None	τ_i	None	—	None	None	None	—
Pseudosecular $S_{1\pm}S_{2\mp}$ unlike	Symmetric dependence on D_M	None	τ_i	Analagous to ω_{EX}	Some dependence on D_M	Reduction analagous to ω_{EX}	No	Yes	Decreases enhancements
Nonsecular									
$S_{1\pm}S_{2z} + S_{1z}S_{2\pm}$	Symmetric dependence on D_M	$[1-\frac{1}{8}(2b\omega_0\tau_i)^{1/2}]$ (lowest order in ω_0) $b = 1$ or 2	$\tau_i[1-\frac{1}{8}(2b\omega_0\tau_i)^{1/2}]$ (lowest order in ω_0)	W_e	Some dependence on D_M	W_e	W_e	Yes	W_e

We exclude in the present discussion any effects from high-frequency and/or large-amplitude modulation of the dc field. They are discussed for ELDOR in Chapter 5. Some discussion of such effects for ENDOR is given in Ref. 29 and Chapter 2.

6.1. *Diagram Method*

An energy level diagram such as the one in Figure 6 for $S = \frac{1}{2}$ and $I = 1$ is constructed.[9] (In this example, ω_e is close to ω_{ab}, and ω_n is close to $\omega_{bd} = \omega_{af}$).

6.1.1. *Forming the Transition Moment Matrix* **d**

a. Draw an arrow between each pair of states for which the energy difference $\hbar\omega_\lambda$ is nearly resonant with an applied radiation field and for which a "transition moment" d_λ or d_η (see below) exists (i.e., the "allowed" transitions). Each arrow should point to the state of increasing quantum number (i.e., the raising convention).

b. An element of the **d** matrix is labeled $d_{\lambda,i}$, where λ represents an induced transition and i is a particular eigenstate. This matrix element is minus (plus) d_λ if λ includes that eigenstate and if the arrow for that transition points toward (away from) the eigenstate. Otherwise it is zero.

c. For an allowed ESR transition near resonance, we have

$$d_\lambda \equiv \tfrac{1}{2}\gamma_e\beta_e\langle -\tfrac{1}{2}, \{M_I\}|S_-|\tfrac{1}{2}, \{M_I\}\rangle \tag{161}$$

where d_λ is the "transition moment" for the λth ESR transition corresponding to a particular nuclear configuration abbreviated as $\{M_I\}$. In a similar manner, we define NMR transition moments

$$d_r \equiv \tfrac{1}{2}\gamma_n B_r[J_r(J_r+1) - M_r(M_r+1)]^{1/2} \tag{162}$$

where the subscript r refers to a particular set of equivalent nuclear spins each of spin I that are "excited" by the rf field, and

$$J_r = \sum_{k \text{ in } r} I_k \qquad \text{with} \qquad J_n = J_r, J_r - 1, \text{ etc.} \tag{163}$$

as allowed by the vector addition of the nuclear spins.

d. Now we introduce the notation that the higher letter is the one of increasing quantum number (i.e., $j > i$ so j is of greater quantum number). Thus if we let λ refer to the $i \leftrightarrow j$ transition, then

$$d_{\lambda,i} = d_{(ij),i} = d_{ij} \tag{164a}$$

$$d_{\lambda,j} = d_{(ij),j} = -d_{ij} \tag{164b}$$

$$d_{\lambda,k} = 0 \qquad \text{for } k \neq i, j \tag{164c}$$

[Note that following the discussion below equation (23′), we need only consider those d_λ, d_η to be nonzero if the λth, ηth transitions are "excited" by the rf field. In the example of Figure 6, $d_{(ab),a} = -d_{(ab),b} = \frac{1}{2}\gamma_e\beta_e$,

$$d_{(bd),b} = -d_{(bd),d} = \tfrac{1}{2}\gamma_n\beta_n\langle 1, 0|J_-|1, 1\rangle = \frac{\sqrt{2}}{2}\gamma_n\beta_n \tag{165a}$$

$$d_{(af),d} = -d_{(af),f} = \tfrac{1}{2}\gamma_n\beta_n\langle 1, -1|J_-|1, 0\rangle = \frac{\sqrt{2}}{2}\gamma_n\beta_n \tag{165b}$$

while all other $d_{\lambda,k}$ are zero.] [Actually equations (162) and (165) represent only the zero-order NMR transition moments, which must, in general, be corrected according to equation (61).]

6.1.2. *Saturation Matrix* **S**

We now use equation (49b) as the definition of the S matrix. It is a matrix in the space of the induced transitions. Consider the $S_{\lambda,\eta}$ element. And let us suppose that λ is the $i \leftrightarrow j$th transition while η is the $k \leftrightarrow l$th transition. Then

$$\begin{aligned} S_{\lambda,\eta} = S_{(ij),(kl)} &= 2\sum_{m,n} d_{(ij),m}(\mathbf{W}^p)^{-1}_{mn} d^{p\,\mathrm{tr}}_{n,(kl)} \\ &= 2d_{ij}d_{kl}[(\mathbf{W}^p)^{-1}_{ik} + (\mathbf{W}^p)^{-1}_{jl} - (\mathbf{W}^p)^{-1}_{il} - (\mathbf{W}^p)^{-1}_{jk}] \qquad \text{for } p \neq i, j, k, l \end{aligned} \tag{166}$$

where we have used the above rules for the **d** matrix. We now introduce the cofactors of W (see the Appendix) to get

$$S_{\lambda,\eta} = \frac{2d_{ij}d_{kl}}{AC}[(C^p_{ki} - C^p_{li}) + (C^p_{lj} - C^p_{kj})], \qquad \text{where } i \neq j \text{ and } p \neq i, j \tag{167}$$

Then, by use of identity (2) of the Appendix [equation (A.22)], we have

$$S_{\lambda,\eta} = \frac{2d_{ij}d_{kl}}{AC}[C^l_{ki} + C^k_{ij}] = \frac{2d_{ij}d_{kl}}{AC}[C^l_{ki} - C^l_{kj}] \tag{168}$$

which by identities (3) and (5) of the Appendix [equation (A.22)], respectively, give

$$\begin{aligned} S_{\lambda,\eta} &= \frac{2d_{ij}d_{kl}}{C}C_{kl,ij} = \frac{2d_{ij}d_{kl}}{C}C_{ij,kl} \\ &\equiv d_{ij}d_{kl}\Omega_{ij,kl} \end{aligned} \tag{169}$$

Now suppose $p = l$. Then $d^{ll'}_{l(rs)} = 0$ for all r, s. Then, instead of equation (166), we have

$$S_{\lambda,\eta} = 2d_{ij}d_{kl}[(W^l)^{-1}_{ik} - (W^l)^{-1}_{jk}]$$
$$= \frac{2d_{ij}d_{kl}}{AC}[C^l_{ki} - C^l_{kj}] = d_{ij}d_{kl}\Omega_{ij,kl} \tag{170}$$

which is the same result as equation (169). These results then prove equation (51).

Note that from identity (5) of the Appendix [equation (A.22)], it follows that $S_{\lambda,\eta} = S_{\eta,\lambda}$ so that the S matrix is symmetric. It also follows from the properties of **d** (viz., there are no nonvanishing transition moments between pairs of states coupled by multiple quantum transition) that there are no elements of S involving multiple quantum transitions; λ and η must each refer to an allowed single-quantum transition.

6.1.3. *Coherence Matrix* **K**

The diagonal elements of **K** are obtained from

$$-[\dot{\sigma} + i(\mathscr{H}_0, \sigma)] \rightarrow \mathbf{K}^{(d)} \tag{171}$$

The only nonvanishing terms are for $\sigma_{\alpha\beta}$, where $E_\alpha \neq E_\beta$ and $\alpha \leftrightarrow \beta$, is an induced transition (not necessarily an allowed transition). The nondiagonal elements of **K** are obtained from:

$$[\varepsilon(t), \sigma] \rightarrow \mathbf{K}^{(n)} \tag{172}$$

where only those terms involving $\sigma_{\alpha\beta}(E_\alpha \neq E_\beta)$ and where $\alpha \leftrightarrow \beta$ is an induced transition need be retained. [The terms diagonal in σ in this equation lead to $\mathbf{d}\dot{\chi} + \mathbf{Q}$ in equation (46a).]

a. Consider those pairs of states connected by an arrow [step (a) for forming the **d** matrix]. Such an arrow represents a single quantum transition corresponding to a steady-state, nonzero value for Z_λ, where Z_λ fulfills the raising convention (see rule 1 for the **d** matrix). For example, in Figure 6, they are $Z_{ba} \equiv Z_e$, $Z_{db} \equiv Z_1$; $Z_{fd} = Z_2$.

b. Now consider all pairs of levels connected by two contiguous arrows (e.g., a and d, b and f in Figure 6). These lead to two quantum transitions, with which are associated nonvanishing Z_λ (e.g., Z_{da} and $Z_{fb} \equiv Z_c$ in Figure 6). The pairs of levels connected by three contiguous arrows are the triple quantum transitions (e.g., Z_{fa}), etc.

c. The diagonal elements of **K** associated with the n-tuple quantum transitions are obtained by adding the $\Delta\omega_\lambda$ for the **n** consecutive single quantum transitions; e.g., $(\omega_n - \omega_{bd}) + (\omega_n - \omega_{df})$ for Z_{fb}.

d. The only off-diagonal elements of **K** for the n-tuple transitions are with $(n-1)$-tuple transitions and with $(n+1)$-tuple transitions, such that the $(n \pm 1)$-tuple transition plus or minus a single quantum transition η equals the n-tuple transition. The matrix element is just $\pm d_\eta$, where the plus (minus) sign is used when the arrow for the η_kth transition points toward (away from) the state in common with the other constituent transition (either an $n-1$ or an n-tuple transition) (e.g., $K_{ba,da} = +d_n$; $K_{db,da} = -d_e$; $K_{da,fa} = +d_n$).

6.1.4. *The* **Q** *Vector*

Q is a vector in the space of induced transitions. Its elements are given simply by

$$Q_\lambda = q\omega_\lambda d_\lambda \tag{173}$$

where, again, $q = \hbar/kTA$, and ω_λ and d_λ are the resonance frequencies and transition moments for the λth transition. Thus, Q_λ is nonzero only for allowed transitions.

6.1.5. *Linewidth Matrix* **R**

The **R** matrix is a matrix in the space of the induced transitions. It is determined by the general expressions for the linewidths (see Section 4.4.2 and Freed and Fraenkel[12]). It is only necessary to include linewidths for those transitions that couple into the problem of interest. This will usually imply that (1) it is some allowed or forbidden transition induced by **d**, and/or (2) it is coupled to such a transition by off-diagonal elements of **R**.

6.2. *Effects of Degenerate States and Transitions*

Very often in ESR spectroscopy, one encounters multiple hyperfine lines resulting from degenerate states. This is often the case if there are several (completely) equivalent nuclei in the radical. (The distinction between equivalent and completely equivalent nuclei is discussed by Freed and Fraenkel.[12]) We shall, for simplicity here, only consider completely equivalent nuclei.) It is then possible to sum over such degeneracies so as to reduce the size of the matrices defined by equations (46) and (48)–(51).[30] Let us refer to a set of completely equivalent nuclei as the rth set and label the degenerate states and transitions by κ corresponding to a particular set of values of the $\{J_r\}$ and $\{M_r\}$. That is, a particular nuclear state is described by the configuration $|\{J_r\kappa\}, \{M_r\kappa\}\rangle$, where for the rth set of equivalent nuclei, the operators $J_r = \sum_{i \text{ in } r} I_i$ and $J_{rz} = \sum_{i \text{ in } r} I_{iz}$, where the sum is over all individual equivalent spins. The curly brackets refer to the collection of J_r

and M_r eigenvalues, respectively, for all the different sets of completely equivalent nuclei. (In the case of a particular NMR transition, we of course mean an $M_r \leftrightarrow M_r \pm 1$ transition). Thus, we define

$$Z_\lambda^{av} \equiv \sum_\kappa Z_{\lambda\kappa} \tag{174a}$$

$$X_\lambda^{av} \equiv \sum_\kappa X_{\lambda\kappa\pm} \tag{174b}$$

which are, respectively, sums over the z components for the λth degenerate transition, and the diagonal density matrix elements (actually their deviations from thermal equilibrium value) for the states between which these transition occur. (Note that we have *not* summed over all transitions, etc., corresponding to a particular hyperfine line regardless of differences in $\{J_r\}$ value. This was discussed in Ref. 30.) It was shown in Ref. 30 that the solution may be rewritten as

$$\mathbf{Z}^{s''} = (\mathbf{M}^s)^{-1}(-\mathbf{R}^s)^{-1}\mathbf{Q}^s \tag{175}$$

with

$$\mathbf{M}^s = \mathbf{1} + (\mathbf{R}^s\mathbf{K}^s)^2 + (-\mathbf{R}^s)^{-1}\mathbf{S}^s \tag{176}$$

and

$$\mathbf{S}^s = 2\mathbf{d}(\mathbf{W}^{J,s})^{-1}\mathbf{d}^{tr\,J} \tag{177}$$

Here,

$$\mathbf{Z}^s \equiv \mathbf{D}^{-1/2}\mathbf{Z}^{av} \tag{178}$$

where $\mathbf{D}^{1/2}$ is a diagonal matrix whose elements are made up from the degeneracies $D(\lambda)$ of the λth transition (corresponding to a particular configuration $\{J_r, M_r\}$).

$$D^{1/2}_{\lambda,\eta} \equiv [D(\lambda)]^{1/2}\,\delta_{\lambda,\eta} \tag{179a}$$

so

$$(\mathbf{D}^{1/2})^{-1}_{\lambda,\eta} \equiv (D^{-1/2})_{\lambda,\eta} = [D(\lambda)]^{-1/2}\,\delta_{\lambda,\eta} \tag{179b}$$

One has $\mathbf{Q}^s = \mathbf{D}^{1/2}\mathbf{Q}$. One also has

$$R^s_{\lambda,\eta} = (R^d_{\lambda,\lambda} - D(\lambda)R^{non}_{\lambda,\lambda})\,\delta_{\lambda,\eta} + R^{non}_{\lambda,\eta}[D(\lambda)D(\eta)]^{1/2} \tag{180}$$

where the diagonal elements $R^d_{\lambda_\kappa,\lambda_\kappa}$ obey

$$R^d_{\lambda_\kappa,\lambda_\kappa} = R^d_{\lambda,\lambda} \tag{181a}$$

for all the κ in λ (since the nuclei are completely equivalent), and the nondiagonal elements $R^{non}_{\lambda_\kappa,\eta_\rho}$, which only come from exchange effects (for the same reason), obey

$$R^{non}_{\lambda_\kappa,\eta_\rho} = R^{non}_{\lambda,\eta} = \omega_{EX}(2/A) \qquad \lambda_\kappa \neq \eta_\rho \tag{181b}$$

Note that for consistency we have

$$[R^{d\,EX}_{\lambda,\lambda} - D(\lambda)R^{non,\,EX}_{\lambda,\lambda}] = -\omega_{EX}[1 - D(\lambda)/\tfrac{1}{2}A] \tag{182}$$

[This was not clearly given in Ref. 30, where the $D(\lambda)$ was left out on the left-hand side.] One also has

$$K^s_{\lambda_\kappa,\eta_\rho} = K_{\lambda,\eta}\,\delta_{\kappa,\rho} \tag{183}$$

In the absence of exchange, one has

$$W^s_{\alpha,\beta} = W_{\alpha,\beta} = W_{\alpha_\kappa,\beta_\rho} \qquad \text{for all } \kappa \text{ and } \rho \tag{184}$$

In the presence of exchange, it is more convenient to go over to the approach based upon equation (147). Then if we assume the sufficiency conditions given above equation (147), we have

$$\hat{W}^s_{\lambda,\eta} = \{[\hat{W}^d_{\lambda,\lambda} - D(\lambda)W^{non,\,EX}_{\lambda,\lambda}]\,\delta_{\lambda,\eta} + \hat{W}^{non,\,EX}_{\lambda,\eta}[D(\lambda)D(\eta)]^{1/2} + \hat{W}^{non,\,END}_{\lambda,\eta}\} \tag{185}$$

where

$$[\hat{W}^{d,\,EX}_{\lambda,\lambda} - D(\lambda)\hat{W}^{non,\,EX}_{\lambda,\lambda}] = 2\omega_{HE}(\tfrac{1}{2} - D(\lambda)/A) \tag{186a}$$

and

$$\hat{W}^{non,\,EX}_{\lambda,\eta} = -2\omega_{HE}/A \tag{186b}$$

(which is also more clearly given than in Ref. 30).

When we use this second approach, then equation (177) becomes

$$\mathbf{S}^s = 4(\hat{\mathbf{d}}, \tilde{\mathbf{d}})\begin{bmatrix}(\hat{\mathbf{W}}^s)^{-1} & \mathbf{0}\\ \mathbf{0} & (\mathbf{W}^{J,s})^{-1}\end{bmatrix}\begin{pmatrix}\hat{\mathbf{d}}^{tr}\\ \tilde{\mathbf{d}}^{tr}\end{pmatrix} = 4[\hat{\mathbf{d}}(\hat{\mathbf{W}}^s)^{-1}\hat{\mathbf{d}}^{tr} + \tilde{\mathbf{d}}(\tilde{\mathbf{W}}^{J,s})^{-1}\tilde{\mathbf{d}}^{tr\,J}] \tag{187}$$

where the submatrices $\hat{\mathbf{d}}$ and $\tilde{\mathbf{d}}$ (as well as $\hat{\mathbf{W}}^s$ and $\tilde{\mathbf{W}}^{J,s}$) are defined in the basis of linear combinations: $\hat{\chi}_\lambda = \chi_{\lambda+} - \chi_{\lambda-}$; $\tilde{\chi}_\lambda = \chi_{\lambda+} + \chi_{\lambda-}$. [Note that the singularities in $\tilde{\mathbf{W}}$ due to equation (29) now appear in $\tilde{\mathbf{W}}$ and it may be treated by the methods of the Appendix.] The construction of $\hat{\mathbf{d}}$ and $\tilde{\mathbf{d}}$ are similar to that of $\mathbf{d}$, and was given explicitly in Ref. 30.

In either approach, we may define the symmetrized saturation parameter by

$$S^s_{\lambda,\eta} \equiv d_\lambda d_\eta \Omega^s_{\lambda,\eta} \tag{188}$$

It then follows from the above, that

$$Z_{\lambda\kappa} = Z_\lambda \qquad \text{independent of } \kappa \text{ in } \lambda \tag{189a}$$

$$\chi_{\lambda\kappa\pm} = \chi_{\lambda\pm} \qquad \text{independent of } \kappa \text{ in } \lambda \tag{189b}$$

so

$$Z^{(s)}_\lambda = D(\lambda)^{1/2}Z_\lambda \tag{189c}$$

and

$$\chi^{(s)}_\lambda = D(\lambda)^{1/2}\chi_\lambda \tag{189d}$$

and we observe, for the λth transition, $Z_\lambda^{sv} = D(\lambda)^{1/2} Z_\lambda^{(s)}$. One may now obtain solutions as in the nondegenerate case.

In the case when equivalent nuclei are not completely equivalent, there will, in general, be off-diagonal couplings due to the END terms in both W and R between degenerate states and ESR transitions belonging to different values of J_r. This complicates the analysis,[6] but by the use of general symmetry arguments[31a] these difficulties may be minimized.*

7. *Average ENDOR and ELDOR*

The general multiple-level problem necessarily involves computer simulations. However, under certain limiting conditions, it is possible to obtain simple analytic expressions. This matter was discussed in detail in Ref. 30. We only wish to summarize the results in their simplest form here. We must make the following assumptions:

1. $\mathbf{K}^s$ is diagonal, i.e., the rf and microwave powers are weak enough that (ENDOR) coherence effects are negligible.

2. $\mathbf{R}^s$ is approximately diagonal (except for exchange coupling of degenerate transitions); i.e., (a) the END terms are not a very large component of the ESR or ENDOR linewidths and (b) ω_{EX} is small enough that the different ESR lines remain well separated.

7.1. *Average ENDOR*

Under the above conditions, it is possible to obtain a simple "average ENDOR" or "average ELDOR" result as though one had the simple four-level systems discussed earlier but with modified parameters. In particular, one has [see equation (78)] for average ENDOR of spins $I = \frac{1}{2}$:

$$E_v = \frac{\xi_{e,v}}{\Omega_{e,v} - \xi_{e,v}} \approx \frac{\xi_{e,v}}{\Omega_{e,v}} \approx \frac{\frac{1}{2} n_v d_{n_v}^2 h(b'') W_e\{0\}^{-2}}{1 + \Delta\omega_{n_v}^2 T_{2,n}^2 + \alpha d_{n_v}^2 b_v h(b'') W_e\{0\}^2} \quad (190)$$

where the vth set of n_v equivalent nuclei are near resonance, and from equation (61), $d_{n_v} = \frac{1}{2}\gamma_n(1 \pm r_n a_{n_v})B_\eta$, where $r_n \equiv (\gamma_e/\gamma_n)(1/2B_0) \approx 1/10$ at X band for protons; $h(b'') = 1 + \frac{1}{2}\omega_{EX}/W_e\{0\}$ $W_e\{0\}$ is the electron spin-flip rate that is independent of quantum number M_v, $b_v = \frac{1}{2} j_{vv}^D(0)/W_e\{0\}$ [see equation (95)]; $T_{2,n_v} \approx [W_e\{0\}h(b'')]^{-1}$. This is the very lowest-order result in the limit that

$$3n_v b_v / h(b'') \ll 1 \quad (191)$$

* Reference 30, footnote 25; and Ref. 31b. One, for example, avoids the problem of pseudotransition probabilities.

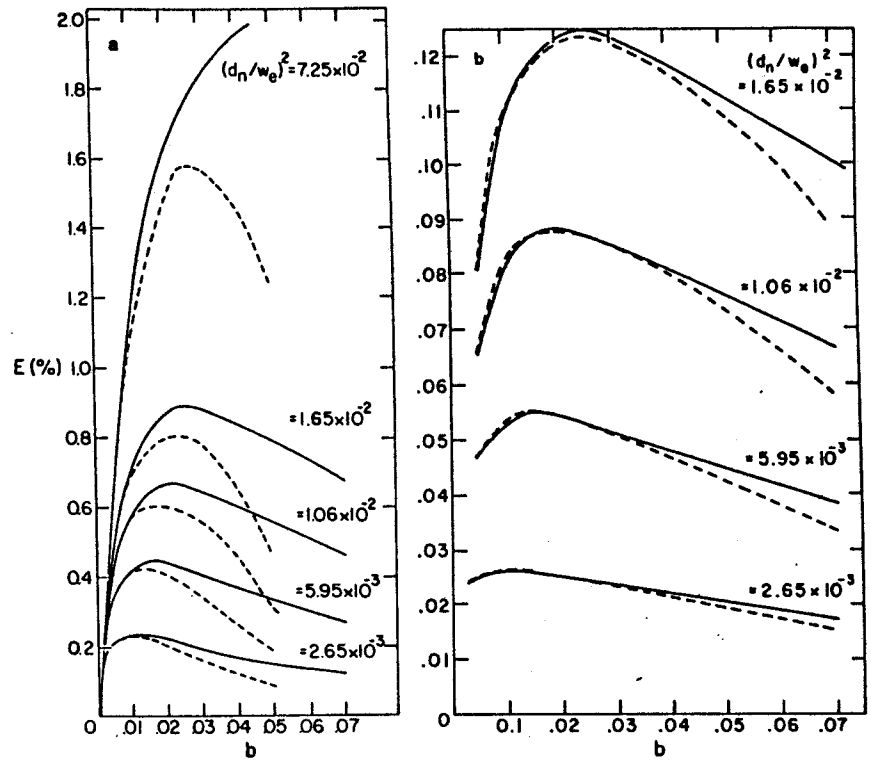

Figure 14. Comparison of the percent enhancements predicted by the average ENDOR approximation (dashed lines) and by the exact solutions (solid lines) for the case of four equivalent spins of $I = \frac{1}{2}$ given as a function of b for different values of $[d_n/W_e(0)]^2$. (a) The $M = 0$ ESR line is saturated, $b'' = 0$, $\Delta\omega_e = \Delta\omega_n = 0$, and $d_e^2 T_{2e}(M)\Omega_e(M) = 1$. (From Freed *et al.*[30]) (b) The $M = 0$ ESR line is saturated, $b'' = 0.08$, $\Delta\omega_e = \Delta\omega_n = 0$, and $d_e^2 T_{2e}(M)\Omega_e(M) = 1$.

The factor $\alpha = 1$ for a radical containing a single set of equivalent nuclei, and in the presence of other equivalent nuclei with small W_{n_r} ($\ll W_{n_v}$), but in the opposite limit of $W_{n_r} \gg W_{n_v}$, it could be reduced to about $\frac{1}{2}$ or $\frac{1}{3}$.[29] Thus, if the NMR transitions are not saturated, i.e., $d_{n_v}^2 \ll b_v h(b'') W_e$, the ratios of the ENDOR peak heights vary as $n_v d_{n_v}^2$ for this case of nuclear spins of $\frac{1}{2}$. In this limit, then, one could determine n_v, which is helpful in assigning the ENDOR transitions. The range of validity of the average ENDOR approach is shown in Figure 14, where the more complete formulas for average ENDOR are compared with the computer-calculated exact results for a case of four equivalent protons. The form of the average ENDOR expressions (e.g., that of a simple four-level system) has been found to be useful also in cases where the detailed average ENDOR theory is not applicable.[29] This is illustrated in

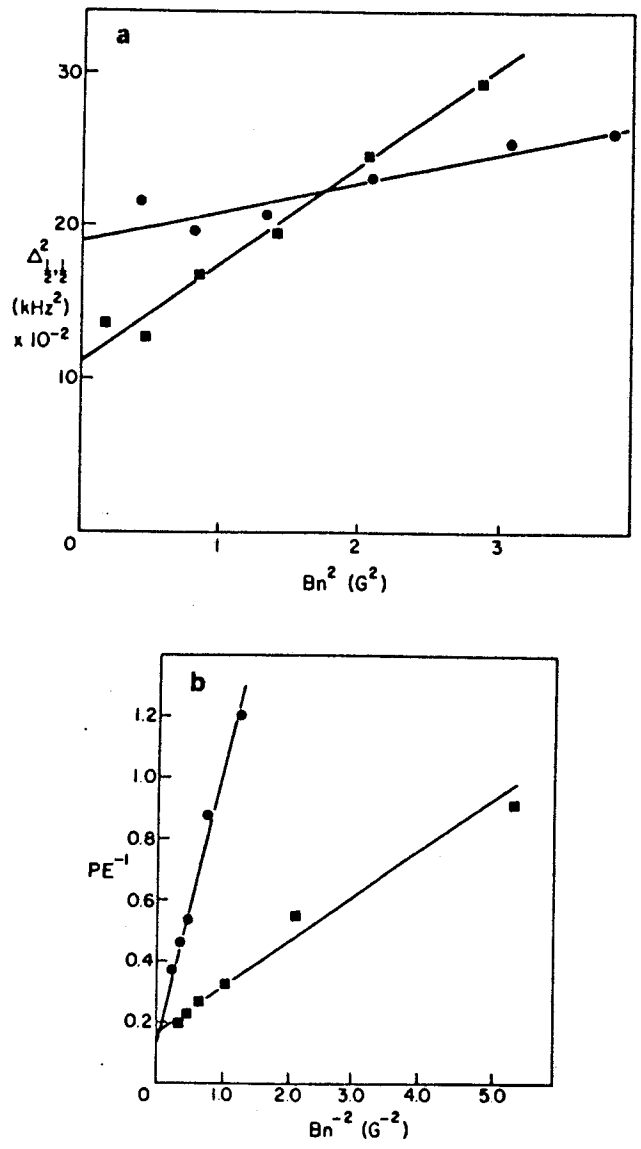

Figure 15. (a) Plots of $\Delta^2_{1/2,\,1/2}$ as a function of B_n^2 (as determined by the rf coherence effect) for PBSQ (●) and DSQ (■) in ethanol at $T = -30°C$. (b) Plot of PE^{-1} as a function of B_n^{-2} (as determined by the rf coherence effect) for PBSQ (●) and DSQ (■) in ethanol at $T = -30°C$.

Figure 15, where, for complex spin systems, the linear dependence of the square of the ENDOR width and the inverse dependence of the ENDOR enhancement on B_n^2 as predicted for the simple case of equations (76)–(78) is shown.

7.2. *Average ELDOR*

In the case of average ELDOR, we consider the results in the limit as $d_p^2 \to \infty$, and $d_o^2 \to 0$, [see equations (59) and (93)]. Then

$$R(d_p^2 \to \infty) \approx \frac{(D_p\{M_r'\})/D_o\{M_r\})^{1/2}\langle\Omega^s_{o,\,p}\{M_r, M_r'\}\rangle}{\langle\Omega^s_p\{M_r'\}\rangle} \tag{192}$$

where the terms in angular brackets are the respective "average" saturation parameters associated with the pumped hyperfine line (nuclear configuration $\{M_r'\}$) and the observing line (nuclear configuration $\{M_r\}$). Then, to lowest order in the b_r and for $I = \frac{1}{2}$, one has

$$R(d_p^2 \to \infty) \approx (D_p\{M_r'\}\frac{\omega_{EX}}{AW_e} + \tfrac{1}{2}\sum_v [b_v/h(b'')][(\tfrac{1}{2}n_v \pm M_v)\delta_{M_v,\,M_v\mp 1}] \tag{193}$$

The $\delta_{M_v,\,M_v\mp 1}$ terms are taken as nonzero only for combinations of $\{M_r\}$ and $\{M_r'\}$ such that only the vth set of equivalent nuclei differ in the observing and pump spin configurations by $\Delta M_v = \pm 1$, and all other sets of equivalent nuclei have the same M_r values. This configuration corresponds to an ELDOR "fundamental line." Overtone ELDOR lines, wherein the $\{M_r'\}$ of the pump line differs more significantly from the $\{M_r\}$ of the observing line, would yield reductions, which come in higher powers of the b_r, and are thus insignificant for $b_r/h(b'') \ll 1$. Thus, in the absence of exchange, in the limits for which average ELDOR applies, only fundamentals will be observed. However, if exchange is dominant, then the ELDOR reduction will depend simply on $D_p\{M_r'\}(\omega_{EX}/AW_e)$ and there are no selection rule restrictions upon which lines are observed or pumped.

8. *Saturation and Double Resonance in the Slow-Tumbling Region*

8.1. *General Considerations*

We would now like to briefly show how the general theory for saturation and multiple resonance in the motional narrowing region may be reformulated to cover the case of slow tumbling. We shall only consider a simple

line for this purpose.[5,32a] Details for multiple lines are given elsewhere.[32-34] The basis for the slow tumbling theory is the stochastic Liouville expression for $\dot{\sigma}(\Omega, t)$[5,33,35-37]:

$$\dot{\sigma}(\Omega, t) = -i[\mathscr{H}_0^x + \varepsilon(t)^x + \mathscr{H}_1(\Omega)^x + iR' - i\Gamma_\Omega][\sigma(\Omega, t) - \sigma_{eq}(\Omega)] \tag{194}$$

Here, Γ_Ω is the Markov operator for the motional process; we will specifically assume it is rotational tumbling, with Ω representing the Euler angles between the fixed laboratory coordinate frame and a molecule-based coordinate frame. Thus, the Euler angles Ω are fluctuating in time. Note that the expression is written for a $\dot{\sigma}(\Omega, t)$, which is both a spin density operator as well as a classical probability function in the values of the random variable Ω. We can recover the ordinary spin density matrix we have used until now by averaging over orientations:

$$\sigma(t) = \int d\Omega\, \sigma(\Omega, t) P_{eq}(\Omega) \equiv \langle P_{eq}(\Omega) | \sigma(\Omega, t) | P_{eq}(\Omega) \rangle \tag{195}$$

where $P_{eq}(\Omega)$ is the equilibrium distribution of orientations and a convenient bra-ket notation is introduced. We have also included in equation (194) a term R', which is that part of the relaxation matrix that is orientation independent.

We note that the Markov operator $\Gamma\Omega$ has associated with it the expression

$$\frac{\partial}{\partial t} P(\Omega, t) = -\Gamma_\Omega P(\Omega, t) \tag{196}$$

where $P(\Omega, t)$ is the probability of finding Ω at a particular state at time t. The process is assumed to be stationary, so that Γ is time independent, and also we have

$$\Gamma_\Omega P_{eq}(\Omega) = 0 \tag{197}$$

We again can make use of equations (14), (15), and (18), for the power absorption, except that now,

$$Z'' = \int d\Omega\, Z(\Omega)'' P_{eq}(\Omega) \tag{198}$$

where

$$Z(\Omega)'' = \sigma_{ba}(\Omega, t) e^{-i\omega t} \tag{199}$$

We now introduce the normalized eigenfunctions of Γ_Ω, the $G_{KM}^L(\Omega)$:

$$\Gamma_\Omega G_{KM}^L(\Omega) = \tau_L^{-1} G_{KM}^L(\Omega) \tag{200}$$

where $\tau_L^{-1} = RL(L+1)$, with R the Brownian rotational diffusion coefficient, which we have assumed is isotropic. Note that $\tau_2 = \tau_R$, which plays the principal role in motional narrowing theory. Also,

$$G_{KM}^L(\Omega) = \left[\frac{(2L+1)}{8\pi^2}\right]^{1/2} \mathscr{D}_{KM}^L(\Omega) \tag{201}$$

where $\mathscr{D}_{KM}^L(\Omega)$ are the Wigner rotation matrices or the generalized spherical harmonics. We then expand in this orthonormal basis set:

$$Z(\Omega) = \sum_{L,K,M} C_{KM}^L G_{KM}^L(\Omega) \tag{202a}$$

$$\chi(\Omega) = \sum_{L,K,M} b_{KM}^L G_{KM}^L(\Omega) \tag{202b}$$

where the C_{KM}^L and b_{KM}^L are expansion coefficients to be solved for. They are, in general, functions of $\Delta\omega$. For an isotropic liquid, $P_{eq}(\Omega) = 1/8\pi^2$, so the ESR signal is proportional to

$$\frac{1}{8\pi^2} \int \mathrm{Im}\, Z(\Omega, \Delta\omega)\, d\Omega = \left(\frac{1}{8\pi^2}\right)^{1/2} \mathrm{Im}\, C_{0,0}^0(\Delta\omega) \tag{203}$$

8.2. *Saturation: A Simple Line*

We now take as our orientation-dependent perturbation[5]

$$\mathscr{H}_1(\Omega) = \mathscr{F} \mathscr{D}_{00}^2(\Omega) S_z \tag{204a}$$

with

$$\mathscr{F} = \tfrac{2}{3}(\beta_e \beta_0/\hbar)(g_\parallel - g_\perp) \tag{204b}$$

That is, we are assuming an axially symmetric g tensor, and we only consider the secular contribution. (The inclusion of the nonsecular contributions is discussed by Freed *et al.*[5]) We now take spin matrix elements of equation (194), as was done in equations (12) and (19). Then we use the eigenfunction expansions given by equation (202), premultiply through these equations by $G_{K'M'}^{L'}(\Omega)^*$, and integrate over Ω.[17] This yields a set of coupled algebraic equations for the C_{KM}^L and the b_{KM}^L:

$$[(\Delta\omega) - i(T_2^{-1} + \tau_L^{-1})] C_{00}^L(\Delta\omega) - \sum_{L'} \kappa_{L,L'} C_{0,0}^{L'}(\Delta\omega) + 2^{1/2} d b_{0,0}^L = q\omega_0 d\delta_{L,0} \tag{205}$$

and

$$-i(T_1^{-1} + \tau_L^{-1}) b_{0,0}^L(\Delta\omega) + 2^{1/2} d\, \mathrm{Im}\, C_{0,0}^L(\Delta\omega) = 0 \tag{206}$$

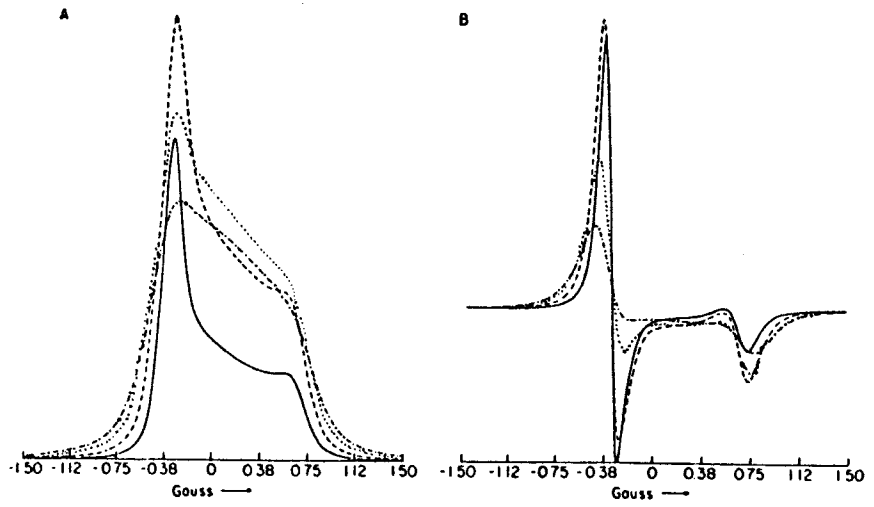

Figure 16. Saturation of single line with rotationally invariant T_1, as a function of B_1 for $|\mathcal{F}|/R = 100$. The different values of $B_1/2$ are 0.01 G (——), 0.025 G (– – –), 0.050 G (···), and 0.75 G (–·–). These correspond to intensity factors of 1414, 1052, 580, and 352, respectively. $g_{\parallel} = 2.00235$, $g_{\perp} = 2.00310$, $T_2 = T_1 = (2W_e)^{-1}$, and $(2/3^{1/2})T_2^{-1}/|\gamma_e| = 0.02$ G. (A) absorption; (B) derivative. (Intensity factor is integrated area under absorption curve in relative units.) (From Freed *et al.*[5])

Here, the orientation-independent T_2^{-1} and T_1^{-1} arise from R', also

$$\kappa_{L,L'} = [(2L+1)(2L'+1)]^{1/2} \begin{pmatrix} L & 2 & L' \\ 0 & 0 & 0 \end{pmatrix} \mathcal{F} \tag{207}$$

where $\begin{pmatrix} L & 2 & L' \\ 0 & 0 & 0 \end{pmatrix}$ is a $3j$ symbol[38] that obeys the triangle rule so that $L' = L$ or $L \pm 2$. All other symbols are as previously defined. We must now solve this coupled set of equations to obtain $\mathrm{Im}\, C^0_{0,0}(\Delta\omega)$ to obtain the spectrum, and this may readily be accomplished on a computer. One merely truncates the coupled equations at a high enough value of L to guarantee convergence. A typical computer simulation is shown in Figure 16.

We can, however, arrange these coupled equations in a convenient matrix array we have seen before by letting

$$(-T_2^{-1} + E_L)\delta_{L,L'} = R_{L,L'} \tag{208a}$$

$$\Delta\omega + \kappa_{L,L'} = K_{L,L'} \tag{208b}$$

also

$$(T_1^{-1} + \tau_L^{-1})\delta_{L,L'} = \hat{W}_{L,L'} \tag{208c}$$

and

$$q\omega_0 d\delta_{L,0} = Q_L \tag{208d}$$

Also, we can introduce a $\hat{\mathbf{d}}$ matrix and a $\hat{\mathbf{d}}^{tr}$ matrix, which by equations (205) and (206) only couple a C^L_{00} with a $b^L_{0,0}$.

In fact, once we make these substitutions we see that we again get the same formal matrix structure as equations (48) and (49), but with equation (49b) replaced by equation (187) and equation (48c) modified accordingly. Also, the $C^L_{0,0}$ form the $\mathbf{Z}$ vector, while the $b^L_{0,0}$ form the $\hat{\chi}$ vector. Note that in the present application, the $\hat{\mathbf{W}}$ matrix is already diagonal, as in the $\mathbf{R}$ matrix. The off-diagonal couplings arise from the $\mathbf{K}$ matrix.

8.3. *ELDOR: A Simple Line*

We can exploit this approach to consider ELDOR on this simple line. Here, we must replace equations (205) and (206) to yield[32]

$$[\Delta\omega_\alpha - i(T_2^{-1} + \tau_L^{-1})]C^L_{0,0}(\alpha) - \sum_{L'} \kappa_{L,L'} C^{L'}_{00}(\alpha) + 2^{1/2} dp b^L_{0,0} = q\omega_e d_\alpha \delta_{L,0} \tag{209}$$

and

$$-i[T_1^{-1} + \tau_L^{-1}]b^L_{0,0} + \sqrt{2} \sum_{\alpha = o,\, p} d_\alpha \, \mathrm{Im} C^L_{0,0}(\alpha) = 0 \tag{210}$$

where $\alpha = o$ or p, referring to observing or pumping signals. The observing absorption line shapes are given by $C^0_{0,0}(0) = C^0_{0,0}(0, \Delta\omega_o, \Delta\omega_p)$. This again yields our standard form for the coupled matrix equations. We show in Figure 17 a computer simulation of such a slow-tumbling ELDOR experiment for this case of a simple line.

The more complex equations one obtains when there are several spin eigenlevels are discussed elsewhere.[32–34] Also, ENDOR in the slow-tumbling region may be treated by similar methods.

The physically new feature here may be appreciated by first realizing that $b^0_{0,0}$, which is the average saturation, is just relaxed by T_1^{-1}, but the $b^L_{0,0}$ for $L > 0$, which represent nonspherically symmetric components of the saturation, are relaxed by the combination $T_1^{-1} + \tau_L^{-1}$; i.e., the rotational motion actually transfers the saturation, which is introduced at one point in the line by the pumping field to other points in the line, which may be observed with a weak observing field. This effect becomes more important as the ratio τ_L^{-1}/T_1^{-1} increases (i.e., the rotational motion slows down).

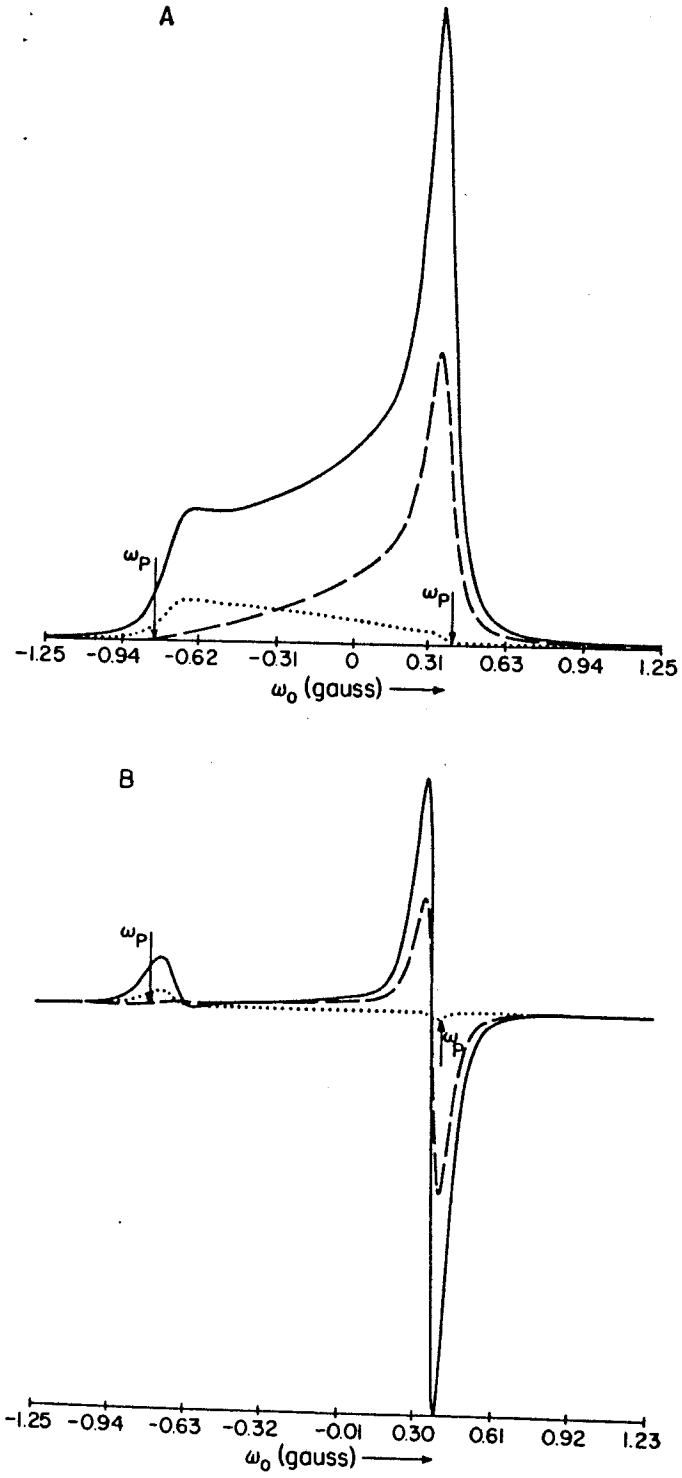

Appendix. General Properties of the Transition Probability Matrix **W**

We first write the cofactor C_{ii} of the **W** matrix:

$$C_{ii} \equiv \begin{array}{c} \\ 1 \\ 2 \\ \\ i \\ \\ \end{array} \begin{vmatrix} 1 & & 2 & & i & \\ \sum_k W_{1k} & \cdots & -W_{12} & \cdots & 0 & \cdots \\ -W_{21} & \cdots & +\sum_k W_{2k} & \cdots & 0 & \cdots \\ \vdots & & \vdots & & \vdots & \\ 0 & \cdots & 0 & \cdots & 1 & \cdots \\ \vdots & & \vdots & & \vdots & \end{vmatrix} \tag{A.1}$$

Add all columns to the jth except the ith and use the property of **W** that the sums of all the columns are zero. Then add all rows to the jth except the ith and use the property of **W** that the sums of all the rows are zero (note **W** is symmetric). Then one has

$$C_{ii} = \begin{array}{c} \\ j \\ \\ \\ \\ i \\ \\ \end{array} \begin{vmatrix} & & & j & & i & \\ \sum_k W_{1k} & -W_{12} & \cdots & W_{1i} & \cdots & 0 & \cdots \\ -W_{21} & \sum_k W_{2k} & \cdots & W_{2i} & \cdots & 0 & \cdots \\ \vdots & \vdots & & \vdots & & \vdots & \\ W_{1i} & W_{2i} & \cdots & \sum_k W_{ki} & \cdots & 0 & \cdots \\ \vdots & \vdots & & \vdots & & \vdots & \\ 0 & 0 & \cdots & 0 & \cdots & 1 & \cdots \\ \vdots & \vdots & & \vdots & & \vdots & \end{vmatrix} \tag{A.2}$$

Figure 17. Observing frequency-sweep ELDOR line shapes for an axially symmetric g tensor undergoing isotropic brownian rotational diffusion with $\tau_R = 2.3 \times 10^{-6}$ sec. (A) absorption, (B) first derivative; (——) pure ESR, (···) pump on and $\omega_p|\gamma_e| = 0.4$ G; (– – –) pump on and $\omega_p|\gamma_e| = -0.8$ G. All have $g_{\parallel} = 2.0235$, $g_{\perp} = 2.00310$, $B_0 = 3300$ G, $T_1^{-1} = 1.76 \times 10^{+5}$ sec^{-1}, $(2/3)^{1/2}T_1^{-1}|\gamma_e| = 0.02$ G. (From Bruno and Freed.[321])

Now permute the ith and jth rows, then the ith and jth columns. It immediately follows that $C_{ii} = C_{jj}$.

Now consider C_{ij}:

$$C_{ij} \equiv \begin{array}{c} \\ j \\ \\ i \\ \\ \end{array} \begin{array}{c} \begin{array}{cccccc} j & & & & i & \end{array} \\ \begin{vmatrix} \sum_k W_{1k} & -W_{12} & \cdots & 0 & -W_{1i} & \cdots \\ -W_{21} & \sum_k W_{2k} & \cdots & 0 & -W_{2i} & \cdots \\ \vdots & \vdots & & \vdots & \vdots & \\ -W_{j1} & -W_{j2} & \cdots & 0 & -W_{ji} & \cdots \\ \vdots & \vdots & & \vdots & \vdots & \\ 0 & 0 & \cdots & 1 & 0 & \cdots \\ \vdots & \vdots & & \vdots & \vdots & \end{vmatrix} \end{array} \tag{A.3}$$

Now add all columns to the ith except the jth. Then

$$C_{ij} = \begin{array}{c} \\ j \\ \\ i \\ \\ \end{array} \begin{array}{c} \begin{array}{cccccc} & & & j & & i \end{array} \\ \begin{vmatrix} \sum_k W_{1k} & -W_{12} & \cdots & 0 & \cdots & W_{1j} & \cdots \\ -W_{21} & \sum_k W_{2k} & \cdots & 0 & \cdots & W_{2j} & \cdots \\ \vdots & \vdots & & \vdots & & & \\ -W_{j1} & -W_{j2} & \cdots & 0 & \cdots & -\sum_k W_{jk} & \cdots \\ \vdots & \vdots & & \vdots & & & \\ 0 & 0 & \cdots & 1 & \cdots & 0 & \cdots \\ \vdots & \vdots & & \vdots & & & \end{vmatrix} \end{array} \tag{A.4}$$

Then exchange the ith and jth columns (an odd permutation) to show that $C_{ij} = C_{ii}$.

It thus follows that

$$C_{ij} = C_{ii} = C_{jj} = C \qquad \text{for all } i \text{ and } j \tag{A.5}$$

$$\therefore \quad |W^k| = \sum_j C_{kj} = AC \tag{A.6}$$

where A is the dimension of $\mathbf{W}$.

We now consider

$$C^i_{jl} \equiv \begin{array}{c} \\ i \\ j \\ \\ \end{array} \begin{array}{c} \begin{array}{cccccc} & & & & l & \end{array} \\ \begin{vmatrix} \sum_k W_{1k} & -W_{12} & \cdots & 0 & \cdots \\ -W_{21} & \sum_k W_{2k} & \cdots & 0 & \cdots \\ \vdots & \vdots & & \vdots & \\ 1 & 1 & \cdots & 0 & \cdots \\ 0 & 0 & \cdots & 1 & \cdots \\ \vdots & \vdots & & \vdots & \end{vmatrix} \end{array} \tag{A.7}$$

and

$$C^l_{il} \equiv \begin{array}{c} \\ i \\ j \\ \\ \end{array} \begin{array}{c} \begin{array}{cccccc} & & & & l & \end{array} \\ \begin{vmatrix} \sum_k W_{1k} & -W_{12} & \cdots & 0 & \cdots \\ -W_{21} & \sum_k W_{2k} & \cdots & 0 & \cdots \\ \vdots & \vdots & & \vdots & \\ 0 & 0 & \cdots & 1 & \cdots \\ \vdots & \vdots & & \vdots & \\ 1 & 1 & \cdots & 0 & \cdots \\ \vdots & \vdots & & \vdots & \end{vmatrix} \end{array} \tag{A.8}$$

Now exchange the ith and jth rows (an odd permutation) of either one to show

$$C^i_{jl} = -C^l_{il} \tag{A.9}$$

We now wish to prove that

$$C_{il}^{k} = C_{jl}^{k} - C_{jl}^{k} \tag{A.10}$$

We start with

$$C_{il}^{k} \equiv \begin{array}{c} \\ k \\ \\ j \\ \\ i \\ \\ \end{array} \begin{array}{c} \begin{array}{cccccccc} & & & k & & l & & i \end{array} \\ \begin{vmatrix} \sum_m W_{1m} & -W_{12} & \cdots & -W_{1k} & \cdots & 0 & \cdots & -W_{1i} & \cdots \\ -W_{21} & \sum_m W_{2m} & \cdots & -W_{2k} & \cdots & 0 & \cdots & -W_{2i} & \cdots \\ \vdots & \vdots & & \vdots & & \vdots & & \vdots & \\ 1 & 1 & & 1 & & 0 & & 1 & \cdots \\ \vdots & \vdots & & \vdots & & \vdots & & \vdots & \\ -W_{j1} & -W_{j2} & \cdots & -W_{jk} & \cdots & 0 & \cdots & -W_{ji} & \cdots \\ \vdots & \vdots & & \vdots & & \vdots & & \vdots & \\ 0 & 0 & & 0 & \cdots & 1 & \cdots & 0 & \cdots \\ \vdots & \vdots & & \vdots & & \vdots & & \vdots & \end{vmatrix} \end{array} \tag{A.11}$$

One now adds all rows to the jth except the kth and ith to obtain

$$C_{il}^{k} = \begin{array}{c} \\ \\ k \\ \\ l \\ \\ i \\ \\ \end{array} \begin{array}{c} \begin{array}{cccccccc} & & & k & & l & & i \end{array} \\ \begin{vmatrix} \sum_m W_{1m} & -W_{12} & \cdots & -W_{1k} & \cdots & 0 & \cdots & -W_{1i} & \cdots \\ -W_{21} & \sum_m W_{2m} & \cdots & -W_{2k} & \cdots & 0 & \cdots & -W_{2i} & \cdots \\ \vdots & \vdots & & \vdots & & \vdots & & \vdots & \\ 1 & 1 & \cdots & 1 & \cdots & 0 & \cdots & 1 & \cdots \\ \vdots & \vdots & & \vdots & & \vdots & & \vdots & \\ W_{l1} + W_{i1} & W_{l2} + W_{i2} & \cdots & -\sum_m W_{lm} + W_{ki} & \cdots & 0 & \cdots & -\sum_m W_{lm} + W_{ki} & \cdots \\ \vdots & \vdots & & \vdots & & \vdots & & \vdots & \\ 0 & 0 & \cdots & 0 & \cdots & 1 & \cdots & 0 & \cdots \\ \vdots & \vdots & & \vdots & & \vdots & & \vdots & \end{vmatrix} \end{array} \tag{A.12}$$

Thus, C_{il}^{k} may be written as the sum of two determinants, in which the first determinant has as it lth row:

$$\left[W_{ki} \quad W_{k2} \quad \cdots \quad -\sum_m W_{km} \quad \cdots \quad 0 \quad \cdots \quad W_{ki} \quad \cdots \right]$$

while the second has as its lth row:

$$\left[W_{i1} \quad W_{i2} \quad \cdots \quad W_{ik} \quad \cdots \quad 0 \quad \cdots \quad -\sum_m W_{im} \quad \cdots \right]$$

while all other elements are as in equation (A.12). Now, by permuting the jth and kth rows of the first determinant, we find that it equals C_{il}^{l}, which, from equation (A.9), is equal to $-C_{jl}^{i}$. Then, by permuting the ith and kth rows of the second determinant, we find that it equals C_{jl}^{k}. It thus follows that $C_{il}^{k} = C_{jl}^{k} - C_{jl}^{i}$. QED

We now wish to prove the relation

$$C_{ki}^{l} - C_{kj}^{l} = AC_{kl,\,ij} \tag{A.13}$$

Let us first consider

$$C_{kj}^{l} \equiv \begin{array}{c} \\ k \\ \\ l \\ \\ \end{array} \begin{array}{c} \begin{array}{cccccc} & & & i & & j \end{array} \\ \begin{vmatrix} \sum_m W_{1m} & -W_{12} & \cdots & -W_{1i} & \cdots & 0 & \cdots \\ -W_{21} & \sum_m W_{2m} & \cdots & -W_{2i} & \cdots & 0 & \cdots \\ \vdots & \vdots & & \vdots & & \vdots & \\ 0 & 0 & \cdots & 0 & \cdots & 1 & \cdots \\ \vdots & \vdots & & \vdots & & \vdots & \\ 1 & 1 & \cdots & 1 & \cdots & 0 & \cdots \\ \vdots & \vdots & & \vdots & & \vdots & \end{vmatrix} \end{array} \tag{A.14}$$

Now add all the columns of C^l_{kj} to the ith except for the jth and then permute the ith and jth columns:

$$C^l_{kj} = \begin{array}{c} \\ k \\ \\ l \\ \end{array} \begin{vmatrix} & & & i & & j & \\ \sum_m W_{1m} & -W_{12} & \cdots & 0 & \cdots & -W_{1j} & \cdots \\ -W_{21} & \sum_m W_{2m} & \cdots & 0 & \cdots & -W_{2j} & \cdots \\ \vdots & \vdots & & \vdots & & \vdots & \\ 0 & 0 & \cdots & 1 & \cdots & 0 & \cdots \\ \vdots & \vdots & & \vdots & & \vdots & \\ 1 & 1 & \cdots & 0 & \cdots & 1-A & \cdots \\ \vdots & \vdots & & \vdots & & \vdots & \end{vmatrix} \tag{A.15}$$

Now consider

$$C^l_{kj} \equiv \begin{array}{c} \\ k \\ \\ l \\ \end{array} \begin{vmatrix} & & & i & & j & \\ \sum_m W_{1m} & -W_{12} & \cdots & 0 & \cdots & -W_{1j} & \cdots \\ -W_{21} & \sum_m W_{2m} & \cdots & 0 & \cdots & -W_{2j} & \cdots \\ \vdots & \vdots & & \vdots & & \vdots & \\ 0 & 0 & \cdots & 1 & \cdots & 0 & \cdots \\ \vdots & \vdots & & \vdots & & \vdots & \\ 1 & 1 & \cdots & 0 & \cdots & 1 & \cdots \\ \vdots & \vdots & & \vdots & & \vdots & \end{vmatrix} \tag{A.16}$$

We now perform the operation $C^l_{ki} - C^l_{kj}$ by simply subtracting the elements of the jth columns of equation (A.15) from (A.16) to obtain

$$C^l_{kl} - C^l_{kj} = \begin{array}{c} \\ k \\ \\ l \\ \end{array} \begin{vmatrix} & & & i & & j & \\ \sum_m W_{1m} & \cdots & -W_{12} & \cdots & 0 & \cdots & 0 \cdots \\ -W_2 & \cdots & \sum_m W_{2m} & \cdots & 0 & \cdots & 0 \cdots \\ \vdots & & \vdots & & \vdots & & \vdots \\ 0 & \cdots & 0 & \cdots & 1 & \cdots & 0 \cdots \\ \vdots & & \vdots & & \vdots & & \vdots \\ 1 & \cdots & 1 & \cdots & 0 & \cdots & A \cdots \\ \vdots & & \vdots & & \vdots & & \vdots \end{vmatrix}$$

$$= A \times k \begin{array}{c} \\ \\ \\ \\ l \\ \end{array} \begin{vmatrix} & & i & & j & \\ \sum_m W_{1m} & -W_{12} & \cdots & 0 & \cdots & 0 \cdots \\ -W_{21} & +\sum_m W_{2m} & \cdots & 0 & \cdots & 0 \cdots \\ \vdots & \vdots & & \vdots & & \vdots \\ 0 & 0 & \cdots & 1 & \cdots & 0 \cdots \\ \vdots & \vdots & & \vdots & & \vdots \\ 0 & 0 & \cdots & 0 & \cdots & 1 \cdots \\ \vdots & \vdots & & \vdots & & \vdots \end{vmatrix} \tag{A.17}$$

$$\equiv AC_{kl,\,ij} = AC_{lk,\,ji} = -AC_{kl,\,ji} = -A_{lc,\,ij} \tag{A.17'}$$

The last equalities follow from simple permutations of equations (A.17). QED

It also follows from equation (A.17) that

$$C_{kl,\,ij} = C_{ij,\,kl} \tag{A.18}$$

because we can interchange rows and columns since W is symmetric.

Another important identity is

$$C_{ik,\,ij} - C_{il,\,ij} = C_{lk,\,ij} \tag{A.19}$$

The proof is as follows. We have from equation (A.13) that

$$AC_{ik,\,ij} = C^k_{ii} - C^k_{ij} \tag{A.20a}$$

$$AC_{il,\,ij} = C^l_{ii} - C^l_{ij} \tag{A.20b}$$

Therefore,

$$\begin{aligned} A(C_{ik,\,ij} - C_{il,\,ij}) &= -(C^l_{ii} - C^k_{ii}) + (C^l_{ij} - C^k_{ij}) \\ &= -C^l_{ki} + C^l_{kj} = -AC_{kl,\,ij} = AC_{lk,\,ij} \end{aligned} \tag{A.21}$$

Furthermore, one may show, utilizing a theorem of Ledermann,[39] that C, $C_{ij,\,ij}$, and $C_{ij,\,ik}$ are always positive quantities, but no *a priori* statement can be made about $C_{ij,\,kl}$ where $i \neq k$, $j \neq l$.

We now summarize these important identities:

$$\begin{aligned}
&(1)\quad C_{ij} = C_{ii} = C_{jj} = C && \text{for all } i, j \\
&(2)\quad C^i_{jl} = -C^j_{il} = C^k_{jl} - C^k_{il}, && i \neq j, k \text{ and } j \neq k \\
&(3)\quad C^l_{ki} - C^l_{kj} = AC_{kl,\,ij}, && l \neq k \text{ and } i \neq j \\
&(4)\quad C_{ik,\,ij} - C_{il,\,ij} = C_{lk,\,ij}, && l \neq k \text{ and } i \neq j, k, l \\
&(5)\quad C_{lk,\,ij} = -C_{lk,\,ij} = C_{lk,\,ji} = C_{ij,\,kl}, && l \neq k \text{ and } i \neq j
\end{aligned} \tag{A.22}$$

Notation

The numbers in parentheses next to each definition represent equation numbers.

a, b, a', b'	Specific eigenstates of spin Hamiltonian (8)
$a, \bar{a}, \bar{a}_n, a(t)$	Isotropic hyperfine splittings; the overbar explicitly indicates a time average, the subscript n indicates the splitting for the nth set of nuclei (42, 61, 120)
a	Hydrodynamic radius of radical of interest (114, 138)
A	Total number of spin eigenstates of spin Hamiltonian $\mathscr{H}_0$ (6)
$\mathbf{A}$	Inverse moment of inertia tensor (114)
b	Dimensionless ratio: W_n/W_e (94′)
b''	Dimensionless ratio: ω_{HE}/AW_e (149′)
$b^L_{km}(\Delta\omega)$	Coefficient in the expansion of $\chi(\Omega)$ in eigenfunctions of the diffusion operator; it is still a function of $\Delta\omega$ (202)
B_1	Strength of the rotating rf or microwave field (1, 11)
B_e, B_p, B_e, B_n	Value of B_1 for observing or pumping mode in ELDOR (41) and the value for the microwave and rf modes in ENDOR (41)
B_0	Strength of the dc magnetic field (27)

$C_{lk} = C$	lkth cofactor of W and is equal to C independent of values of l and k (34, 37)
$C_{ij,\,kl}$	Double cofactor of W (35)
C^l_{kl}	kith cofactor of $\mathbf{W}^l$ (36)
C	Spin-rotational constant of the radical (113)
$C^L_{KM}(\Delta\omega)$	Coefficient in the expansion of $Z(\Omega)$ in eigenfunctions of the diffusion operator; it is still a function of $\Delta\omega$ (202)
$d = \frac{1}{2}\gamma_e B_1$	Induced transition moment due to applied rf or microwave field (13)
$d_e, d_p, d_e, d_n, d_\lambda$	Value of d for observing or pumping mode in ELDOR (44) and the value for the microwave and rf modes in ENDOR (61, 64); λ represents the value of d for the λth induced transition (173)
d_{n_0}	Nuclear spin transition moment neglecting the high-field correction (61)
d_n^{crit}	Critical value of d_n for coherence splittings in ENDOR (83)
$\mathbf{d}, \mathbf{d}^{\text{tr}}$	Matrix of transition moments and its transpose (46)
$\hat{\mathbf{d}}, \tilde{\mathbf{d}}$	Partitioned components of $\mathbf{d}$ (187)
d	Interaction distance for exchange (138)
$D^{(m)}$	mth irreducible-tensor component of the electron–nuclear dipolar coefficients (105)
D	Coefficient for translational diffusion of a radical (138)
$D(\lambda)$	Degeneracy of the λth transition (140)
$\mathbf{D}^{1/2}$	Diagonal matrix whose elements are the $[D(\lambda)]^{1/2}$ (178)
$\mathscr{D}^L_{KM}(\Omega)$	Generalized spherical harmonics (Wigner rotation matrices) (201)
E	Enhancement factor in ENDOR (78)
f	Debye–Hückel correction to rate of bimolecular collisions (138)
$\mathscr{F} = \frac{2}{3}(\beta_e B_0/h)(g_\parallel - g_\perp)$	(204)
$\mathbf{g}, \Delta\mathbf{g}$	g tensor and deviation of g tensor from free electron value g_e [below (114)]
$g_n, \bar{g}_n$	g factor equal to Tr g. The overbar explicitly indicates a time average (111, 125)
$g_k, g_\parallel, g_\perp, g^{(m)}$	g tensor components $k = x$, y, or z in its principal axis system, $g_\parallel = g_z$ and $g_\perp = g_x = g_y$ for axial symmetry; $g^{(m)}$ are irreducible tensor components of g (111, 112, 125)
$G^L_{km}(\Omega)$	Normalized eigenfunctions of Γ_Ω, the diffusion operator (200)
$h(b'')$	$= 1 + \frac{1}{2}\omega_{EX}/W\{0\}$ (190)
$\mathscr{H}_0, \mathscr{H}^x_0$	Zero-order spin Hamiltonian, and the superscript x indicates the superoperator form, e.g., $\mathscr{H}^x_0\sigma = [\mathscr{H}_0, \sigma]$ (5, 131)
$\mathscr{H}_1(t), \langle\mathscr{H}_1(t)\rangle, \mathscr{H}^x_1$	Randomly modulated perturbation term in the spin Hamiltonian, its ensemble averaged value, and its superoperator form [below (27, 123, 194)]
$\mathscr{H}_J, \mathscr{H}^x_J$	Heisenberg spin-exchange term in the spin Hamiltonian and its superoperator form (132, 133)
I	Nuclear spin quantum number for single nucleus [above (85)]
$\mathbf{I}$	moment of inertia of radical (113)
$j^D(\omega), j^{G_2}(\omega), j^{DG_2}(\omega), j^Q(\omega), j^I(\omega), J^{G_0}(\omega), J^{IG_0}(\omega)$	Spectral density as a function of ω from random modulation of: D, electron–nuclear dipolar interaction (END) (103); G_2, g tensor (111); DG_2, cross-term between END and g tensor (112); Q, quadrupolar interaction (106); I, isotropic dipolar (118); G_0, g shift (125); IG_0, cross-term between isotropic dipolar and g-shift (126)
J	Total nuclear spin quantum number for group of equivalent nuclear spins [above (65)]

J Twice the exchange integral (133)
k Boltzmann's constant (6)
$\mathbf{K}, \mathbf{K}^s$ Coherence matrix and its symmetrized form in the presence of degenerate transitions (46, 176)
L Principal quantum number for generalized spherical harmonics (200)
M_0 Equilibrium magnetization (1)
$M_x, M_y, M_\pm = M_x \pm iM_y$ Components of magnetization in the laboratory frame (2)
$\tilde{M}_x, \tilde{M}_y$ Components of magnetization in the rotating frame (1)
M_s Quantum number for projection of electron spin on z axis (8)
M, M_a, M_b Quantum number for projection of nuclear spin on z axis; the subscripts a or b refer to the ath or bth spin state [above (103, 124)]
$\{M_I\}$ A particular configuration of the nuclear spin states in a multinuclear spin problem (161)
$\mathbf{M}, \mathbf{M}^s$ Basic matrix in the solution of multiple resonance; the superscript s indicates the symmetrized form in the presence of degeneracies (49, 175)
$\mathscr{M}_\pm$ Quantum mechanical operator for the magnetization (3)
n_υ Number of equivalent nuclei in the υth set of equivalent nuclei (190)
$\mathscr{N}$ Concentration of radicals with electron spin $S = \frac{1}{2}$ (3)
P Power absorbed from the resonant field (14)
P_i Population of the ith state $= \sigma_{ii}$ [below (59)]
$P(\Omega, t), P_{eq}(\Omega)$ Classical time-dependent distribution function for orientation of radical and its time-independent equilibrium value (195, 196)
$\mathscr{P}, \mathscr{P}^x$ Operator that permutes electron spins and its superoperator form (135–137)
$q = \hbar/kTA$ (24)
$\mathbf{Q}$ Vector, in transition space, of the driving terms (47)
eQ Quadrupole coupling constant (107)
r' Radial distance of the unpaired electron with respect to a nucleus (105)
r_n Dimensionless parameter measuring importance of high-field correction to d_n [below (190)]
$R, R_{\alpha\alpha'\beta\beta'}$ Relaxation matrix and its general four-indexed matrix element (5)
$R_{ba,ba}, R_{\lambda\lambda} = R_\lambda$ Diagonal element of relaxation matrix for the linewidth of the transition between states a and b (10); also its general form for the λth transition (180)
$R_{bb,aa}, R_{aa,aa}$ Relaxation matrix elements that yield the transition probabilities (19)
$\mathbf{R}, \mathbf{R}^s, R_{\lambda,\eta}$ Matrix yielding the (coupled) linewidths, its symmetrized form, and the matrix element coupling the λth and ηth transitions (46, 175, 180)
R Reduction factor in ELDOR (93)
R' That part of the relaxation matrix R that does not arise from rotational tumbling (194)
R Rotational diffusion coefficient (200)
$S_\pm$ Raising and lowering operators for the electron spin (4)
$\mathbf{S}, \mathbf{S}^s, \mathbf{S}_{\lambda,\eta}$ Saturation matrix, its symmetrized form, and the matrix element coupling the λth and ηth transitions (49, 51, 176)
t Time (2)

T Kelvin temperature (6)
T_1 Longitudinal spin–relaxation time for a simple two-level spin system (1)
$T_2^{-1}, T_{2e}^{-1}, T_{2p}^{-1}, T_e^{-1}, T_n^{-1}, T_x^{-1}$ Simple linewidths contained in $\mathbf{R}$, where o and p are for observing and pumping transitions and e, n, and x are for electron spin, nuclear spin, and cross-transitions, and the subscript 2 is often dropped (1, 44, 64)
$T_{2ab} - 1$ Secular contribution to the linewidth for the transition between states a and b (122)
$\mathrm{Tr}, \mathrm{Tr}_s$ Trace over spin states (and symmetrized trace for interacting dimers) (4, 13)
$\mathbf{U}, U_a$ A vector and its element as used in solving for the saturation of a simple line (30)
$\mathbf{U}^l$ Obtained from $\mathbf{U}$ by replacing the lth element by zero (30′)
V_{ba} Line-shape term for simple transition between a and b (31)
V'_{ij} V is the electrostatic potential at the nucleus and V'_{ij}, $i, j = x', y'$, or z', indicates differentiation of V with respect to i and j (108)
W_{ab}, Wa_γ Transition probability from state b to state a (and from arbitrary state γ to state a) leading to spin relaxation (20)
W_e, W_n, W_x Transition probabilities for: e, pure electron spin flips; n, pure nuclear spin flips; and x, combined electron spin and nuclear spin flips; cross-transitions (26, 93)
$W_e^{SR}, W_e\{0\}$ Spin-rotational contribution to W_e and the value of W_e for electron spin flips in the nuclear configuration specified by $\{0\}$ (109, 190)
$\mathbf{W}, \mathbf{W}^l, \mathbf{W}^{l,s}$ Transition probability matrix; the modified transition probability matrix obtained by replacing the lth row of $\mathbf{W}$ with ones; the symmetrized form of $\mathbf{W}^l$ when one sums over degenerate states (30, 30′, 177)
$\hat{\mathbf{W}}, \tilde{\mathbf{W}}, \hat{\mathbf{W}}^s, \tilde{\mathbf{W}}^s$ Partitioned submatrices of a rearranged $\mathbf{W}$ and their symmetrized forms when one sums over degenerate states (147, 187)
$Y_{2,m}(\theta', \phi')$ Second-rank spherical harmonics (105)
$Z = Z' + iZ'', Z^*$ Function describing the induced transition, where Z' is the dispersive component while Z'' is the absorptive component and Z^* is the complex conjugate (15, 17, 18, 26)
Z''_o, Z''_p Absorptive components for observing and pumping modes in ELDOR (44, 45)
Z''_{ENDOR}, Z''_{ESR} Absorptive components in presence and absence of resonant NMR field in ENDOR (78)
$\mathbf{Z} = \mathbf{Z}' + i\mathbf{Z}''$ Vector of induced transitions (46)
$\mathbf{Z}^{s\nu}, \mathbf{Z}^s$ Vector of elements $Z_\lambda^{s\nu}$ involving a sum over all κ elements of $Z_{\lambda\kappa}$ belonging to the λth degenerate transition; $\mathbf{Z}^s$ is the symmetrized form of $\mathbf{Z}^{s\nu}$ (174, 178)
$\alpha, \alpha', \beta, \beta'$ Arbitrary spin states (5b)
α Correction factor in average ENDOR (190)
β_e Bohr magneton (111)
γ_e, γ_n Gyromagnetic ratio: e, electronic; n, nuclear (1, 60)
Γ_Ω Markovian (diffusion) operator for the motional process (194)
$\Delta_e \equiv \Delta\omega_e, \Delta_n \equiv \Delta\omega_n$ (62)
$\varepsilon(t)$ Term in the spin Hamiltonian that includes the interaction of the spins with the oscillating fields (5)
$[\nabla\varepsilon]^{(m)}$ Irreducible tensor components of the electric-field gradient (108)
η Solvent viscosity (114)

θ' Polar angle for defining the orientation in the molecular frame of the radial vector from the nucleus to the unpaired electron distribution (105)

κ Label of degenerate nuclear spin states corresponding to the same value of J and M [above (103)]

$\kappa_{L,L'}$ L, L'th matrix element for "coherence matrix" in slow tumbling (205)

ξ_e Term representing effect of ELDOR on observing ESR signal for simple case (54)

ξ_e, ξ_e^r Term representing effect of ENDOR on observing ESR signal for simple case; superscript r implies the NMR transition is exactly on resonance (69, 75)

ρ Spin-density matrix for an interacting pair of dimers (131)

$\sigma(t), \sigma_{\alpha\alpha'}, \sigma^*_{\alpha\alpha'}$ Spin-density matrix for the radicals, the α–α'th matrix element, and its Hermitian conjugate (3, 5, 17)

$\sigma_{eq}, \sigma_{eq,\alpha\alpha'}$ Equilibrium spin-density matrix and its $\alpha\alpha'$th matrix element (5)

$\sigma(\Omega, t)$ Combined molecular classical orientation distribution function and spin-density matrix (194)

$\sigma_{eq}(\Omega)$ Equilibrium value of $\sigma(\Omega, t)$ (194)

τ_c Correlation function for random process (27)

τ_R, τ_L Correlation functions for rotational reorientation (104, 200)

τ_J Correlation function for angular momentum relaxation (113)

τ_1 Mean lifetime of interacting radical pairs (132)

τ_2 Mean time between bimolecular encounters (131)

ϕ' Azimuthal angle for defining the orientation in the molecular frame of the radial vector from the nucleus to the unpaired electron distribution (105)

χ, χ_a Deviation of σ from σ_{eq} and its diagonal element for state a (222)

χ Column vector of elements χ_l (30)

$\chi_{a\pm}, \chi_\pm$ Value of χ for state $M_s = \pm$ and $\{M_I\} = \alpha$; also $\chi_\pm$ is a normalized sum of $\chi_{a\pm}$ (142, 143)

$\hat{\chi}$ A partitioned subvector of χ whose λth element equals $\chi_{\lambda+} - \chi_{\lambda-}$ [(142), below (187)]

$\chi^{a\nu}_{\lambda\pm}$ Sum over all κ elements of $\chi_{\lambda\kappa\pm}$ belonging to the same degenerate state. $\lambda_\pm$ (174)

ψ_e Electronic wave function of the unpaired electron (105)

$\omega_{\alpha\alpha'}; \omega_\lambda$ Larmor frequency for $\alpha \leftrightarrow \alpha'$ transition and for λth transition (5, 173)

ω_0 Larmor frequency for ESR transition (12)

ω_e, ω_p Frequency of applied observing and pumping microwave fields in ELDOR (44)

ω_e, ω_n Frequency of applied ESR and NMR fields in ENDOR (62)

$\omega^{a,b}(t)$ Fluctuating component of frequency difference between states a and b (122)

ω_{HE}, ω_{EX} Heisenberg exchange frequency and general exchange frequency including both Heisenberg exchange and chemical exchange [(135), below (144)]

$\Delta\omega \equiv \omega - \omega_e$ $= \omega - \omega_0$, with ω the applied microwave frequency (1, 16, 44)

$\Delta\omega_i = \omega_i - \omega_\lambda$ Difference between frequency of ith rotating field and Larmor frequency for λth transition that is nearly resonant with ω_i [below (173)]

$\Delta\omega_e, \Delta\omega_p$ Near-resonant frequency difference for observing and pumping fields in ELDOR (44)

$\Delta\omega_e, \Delta\omega_n$ Near-resonant frequency difference for ESR and NMR fields in ENDOR (see Δ_e, Δ_n)

$\Omega_{ij,kl}\Omega_{\lambda,\eta}$ General saturation parameter coupling the $(i \leftrightarrow j)$th transition to the $(k \leftrightarrow l)$th transition and coupling the λth and ηth transitions (35, 41)

$\Omega_{ba,ba} = \Omega_{ba}$ Diagonal saturation parameter, which plays a role related to T_1 for steady-state saturation of the $a \leftrightarrow b$ transition (31, 39)

Ω Euler angles defining the transformation between laboratory and molecular coordinate frames (194)

ACKNOWLEDGMENT

We wish to thank NSF for partial support of this work through grants no. CHE-75-00938 and CHE-77-26996.

References

1. A. Abragam, *The Principles of Nuclear Magnetism.* Oxford University Press, London (1961).
2. A. G. Redfield, *Adv. Mag. Res.* **1**, 1 (1965).
3. J. H. Freed, *J. Chem. Phys.* **49**, 376 (1968).
4. L. T. Muus and P. W. Atkins (eds.), *Electron-Spin Relaxation in Liquids*, Plenum Press, New York (1972).
5. J. H. Freed, G. V. Bruno, and C. F. Polnaszek, *J. Phys. Chem.* **75**, 3385 (1971).
6. J. H. Freed, *J. Chem. Phys.* **43**, 2312 (1965).
7. J. H. Freed, *J. Phys. Chem.* **71**, 38 (1967).
8. J. S. Hyde, J. C. W. Chien, and J. H. Freed, *J. Chem. Phys.* **48**, 4211 (1968).
9. J. H. Freed, D. S. Leniart, and J. H. Freed, *J. Chem. Phys.* **47**, 2762 (1968).
10. J. H. Freed, *J. Chem. Phys.* **50**, 2271 (1969).
11. G. Rist and J. H. Freed, unpublished results.
12. J. H. Freed and G. K. Fraenkel, *J. Chem. Phys.* **39**, 326 (1963).
13. P. W. Atkins, in *Electron-Spin Relaxation in Liquids* (L. T. Muus and P. W. Atkins, eds.), Chapter XI, Plenum Press, New York (1972).
14. G. K. Fraenkel, *J. Phys. Chem.* **71**, 139 (1967).
15. J. H. Freed, *J. Chem. Phys.* **41**, 2077 (1964).
16. J. H. Freed and G. K. Fraenkel, *J. Chem. Phys.* **41**, 3623 (1964).
17. J. H. Freed, in *Electron-Spin Relaxation in Liquids* (L. T. Muus and P. W. Atkins, eds.), Chapters VIII and XVIII, Plenum Press, New York (1972).
18. D. Kivelson, in *Electron-Spin Relaxation in Liquids* (L. T. Muus and P. W. Atkins, eds.), Chapter X, Plenum Press, New York (1972).
19. G. R. Luckhurst, in *Electron-Spin Relaxation in Liquids* (L. T. Muus and P. W. Atkins, eds.), Chapter XV, Plenum Press, New York (1972).
20. S. A. Goldman, G. V. Bruno, C. F. Polnaszek, and J. H. Freed, *J. Chem. Phys.* **56**, 716 (1972).
21. J. S. Hwang, R. P. Mason, L. P. Hwang, and J. H. Freed, *J. Phys. Chem.* **79**, 489 (1975).
22. C. F. Polnaszek and J. H. Freed, *J. Phys. Chem.* **79**, 2283 (1975).

23. J. H. Freed, *J. Chem. Phys.* **66**, 4183 (1977).
24. M. P. Eastman, R. G. Kooser, M. R. Das, and J. H. Freed, *J. Chem. Phys.* **51**, 2690 (1969).
25. M. P. Eastman, G. V. Bruno, and J. H. Freed, *J. Chem. Phys.* **52**, 321 (1970).
26. J. I. Kaplan, *J. Chem. Phys.* **28**, 278, 462 (1958); S. Alexander, *J. Chem. Phys.* **37**, 966, 974 (1962).
27. J. H. Freed, in *Chemically-Induced Magnetic Polarization* (L. T. Muus, T. W. Atkins, K. A. McLauchlin, and J. B. Pedersen, eds.), Chapter 19, D. Reidel, Dordrecht, Holland (1977).
28. S. A. Goldman, J. B. Pedersen, and J. H. Freed, to be published.
29. D. S. Leniart, H. D. Connor, and J. H. Freed, *J. Chem. Phys.* **63**, 165 (1975).
30. J. H. Freed, D. S. Leniart, and H. D. Connor, *J. Chem. Phys.* **58**, 3089 (1973).
31a. N. C. Pyper, *J. Mol. Phys.* **21**, 1 (1971); **22**, 433 (1971); B. C. Sanctuary, *J. Chem. Phys.* **64**, 4352 (1976).
31b. J. H. Freed, unpublished results.
32a. G. V. Bruno and J. H. Freed, *Chem. Phys. Lett.* **25**, 328 (1974).
32b. G. V. Bruno, Ph.D. Thesis, Cornell University, Ithaca, New York (1973).
33. J. H. Freed, *J. Phys. Chem.* **78**, 1155 (1974).
34. J. S. Hyde, M. D. Smigel, L. R. Dalton, and L. A. Dalton, *J. Chem. Phys.* **62**, 1655 (1975).
35. J. H. Freed, *Ann. Rev. Phys. Chem.* **23**, 265 (1972).
36. A. J. Vega and D. Fiat, *J. Chem. Phys.* **60**, 579 (1974).
37. L. P. Hwang and J. H. Freed, *J. Chem. Phys.* **63**, 118 (1975).
38. A. R. Edmonds, *Angular Momentum in Quantum Mechanics*. Princeton University Press, Princeton, New Jersey (1957).
39. W. Ledermann, *Proc. Cambridge Phil. Soc.* **46**, 581 (1950).

4

Solution ENDOR

Neil M. Atherton

1. *Introduction*

ENDOR is one of the oldest double resonance techniques, the first experiments on solids having been reported by Feher in 1956.[1] In fluid solutions, the nuclear spin relaxation times are shorter than in solids, and higher radiofrequency powers are required to observe ENDOR, for the nuclear transitions must be driven at a rate comparable to that due to relaxation. This requirement makes the instrumentation for solution ENDOR more difficult than that for solids and explains, at least to some extent, why the application of the technique to solutions has lagged somewhat behind that to solids.

The first solution ENDOR signals were obtained by Cederquist from metal–ammonia solutions.[2] Unfortunately, this work has never been published in the conventional sense and so is probably not as widely known and discussed as it deserves. It was not until 1964 that Hyde and Maki[3] reported signals from free radicals in solution, with a fuller account describing the spectrometer and results for a range of systems appearing a year later.[4] Since that time, the field has expanded steadily but quite slowly. A fair assessment of the present state of affairs is probably that solution ENDOR is well established and reasonably well understood, but there are many applications yet to be perceived and made. It would be surprising if experiments still to be done did not yield some unlooked-for results.

In ENDOR, one monitors the level of an ESR absorption and records the change in it when a nuclear resonance transition is driven by a second

Neil M. Atherton • Department of Chemistry, The University of Sheffield, Sheffield, England